

ISSN 8755-6839

SCIENCE OF TSUNAMI HAZARDS

The International Journal of The Tsunami Society
Volume 27 Number 4 Published Electronically 2008

UNDERSTANDING TSUNAMI RISK TO STRUCTURES: A CANADIAN PERSPECTIVE
D. Palermo and I. Nistor - *Dept. of Civil Engineering, University of Ottawa, Ottawa, CANADA.* 1

MINIMIZING COMPUTATIONAL ERRORS OF TSUNAMI WAVE-RAY AND TRAVEL TIME
Andrei G. Marchuk - *Institute of Computational Mathematics and Mathematical Geophysics, Siberian Division, Russian Academy of Sciences, Novosibirsk, RUSSIA.* 12

ASSESSMENT OF THE IMPACT OF THE TSUNAMI OF DECEMBER 26, 2004 ON THE NEAR-SHORE BATHYMETRY OF THE KALPAKKAM COAST, EAST COAST OF INDIA
C. Anandan* and P. Sasidhar - *Safety Research Institute, Atomic Energy Regulatory Board, Govt. of India, Kalpakkam INDIA* 26

TSUNAMI MITIGATION IN HAWAII
George D. Curtis - *University of Hawai'i, Department of Ocean and Resource Engineering, 2450 Dole St., Honolulu HI. USA.* 36

OBSERVED INFERENCES FROM SUDDEN CHANGES IN THE SEDIMENTOLOGICAL PROCESSES DURING THE DECEMBER 26, 2004 TSUNAMI ALONG THE EAST COAST OF INDIA 43

Loveson, V. J. - Central Institute of Mining & Fuel Research, Dhanbad. *INDIA*

Angusamy, N. - Tamil University, Thanjavur. *INDIA*

Gujar, A. R. - Geolog. Oceanography Div, National Inst. of Oceanography, Dona Paula, Goa, *INDIA*

Chandrasekar, N. - Centre for Geotechnology, Manonmaniam Sundaranar Univ, Abishekhapatti, Tirunelveli, *INDIA*

Rajamanickam, G. V. - Dept of Disaster Management, SASTRA University, Thanjavur, *INDIA*

Copyright © 2008 - THE TSUNAMI SOCIETY

THE TSUNAMI SOCIETY

P. O. Box 2117, Ewa Beach, HI 96706-0117, USA,

WWW.TSUNAMISOCIETY.ORG

OBJECTIVE: The Tsunami Society publishes this journal to increase and disseminate knowledge about tsunamis and their hazards.

DISCLAIMER: Although these articles have been technically reviewed by peers, the Tsunami Society is not responsible for the veracity of any statement, opinion or consequences.

EDITORIAL STAFF

Dr. George Pararas-Carayannis, Editor
1741 Ala Moana Blvd. No 70, Honolulu, Hawaii 96815, USA.

<mailto:drgeorgepc@yahoo.com>

EDITORIAL BOARD

Dr. Charles MADER, Mader Consulting Co., Colorado, New Mexico, Hawaii, USA
Dr. Hermann FRITZ, Georgia Institute of Technology, USA
Prof. George CURTIS, University of Hawaii -Hilo, USA Dr. Tad S. MURTY, Ottawa, Canada
Dr. Zygmunt KOWALIK, University of Alaska, USA
Dr. Galen GISLER, Norway
Prof. Kam Tim CHAU, Hong Kong Polytechnic University, Hong Kong
Dr. Jochen BUNDSCHUH, (ICE) Costa Rica, Royal Institute of Technology, Stockholm, Sweden
Dr. Yurii SHOKIN, Novosibirsk, Russian Federation

TSUNAMI SOCIETY OFFICERS

Dr. George Pararas-Carayannis, President; Dr. Tad Murty, Vice President; Dr. Gerard Fryer, Secretary; Dr. Vindell Hsu, Acting Treasurer.

Submit manuscripts of articles, notes or letters to the Editor. If an article is accepted for publication the author(s) must submit a scan ready manuscript, a Doc, TeX or a PDF file in the journal format. Issues of the journal are published electronically in PDF format. Recent journal issues are available at:
<http://www.TsunamiSociety.org>
<http://www.sthjournal.org>

Tsunami Society members will be advised by e-mail when a new issue is available. There are no page charges for one paper per calendar year for authors who are members of the Tsunami Society. Permission to use figures, tables and brief excerpts from this journal in scientific and educational works is hereby granted provided that the source is acknowledged.

Issues of the journal from 1982 thru 2005 are available in PDF format at
<http://epubs.lanl.gov/tsunami/> and on a CD-ROM from the Society to Tsunami Society members. ISSN 8755-6839 <http://www.sthjournal.org>

UNDERSTANDING TSUNAMI RISK TO STRUCTURES: A CANADIAN PERSPECTIVE

D. Palermo¹ and I. Nistor¹

¹ *Assistant Professor, Dept. of Civil Engineering , University of Ottawa, Ottawa, Canada
Email: palermo@eng.uottawa.ca, inistor@uottawa.ca*

ABSTRACT

The potential catastrophic effects of tsunami-induced loading on built infrastructure in the vicinity of shorelines have been brought to the fore by recent global events. However, state-of-the-art building codes remain silent or provide conflicting guidance on designing near-shoreline structures in tsunami-prone areas. This paper focuses on tsunami-induced loading and its effect on structures within the Canadian context. The mechanics of tsunami-induced loading is described based on knowledge gained during reconnaissance visits after the 2004 south-east Asia Tsunami, as well as post-construction visits to countries significantly affected by the destructive forces of the tsunami. To gain an appreciation of the magnitude of tsunami-induced bores for a given seismic event along the western coastal region of Canada, structural analysis of a simple near-shoreline structure was performed considering a proposed loading protocol for tsunami-induced hydraulic bores. These loads were further compared to seismic loading in order to provide an estimation of the tsunami risk and its impact. The work was complemented by experimental results from a large-scale testing program conducted with the purpose of estimating the forces experienced on structural components. Square-, rectangular-, and diamond-shaped columns were used to study the influence of shape. Furthermore, results from debris impact testing are also discussed.

KEYWORDS: Tsunami, structures, hydrodynamics, surge, debris impact, loading combinations

1. INTRODUCTION

As awareness of the significant threat of tsunami loading on coastal and near coastal structures increases, so too does the need for guidance for engineers involved in designing structures located near coastlines, in high risk tsunami-prone areas. The National Building Code of Canada (NBCC 2005) does not provide, for the most part, guidelines for the design for tsunami-induced effects. Commentary J, "Design for Seismic Effects," states that damage to buildings as a result of an earthquake can arise from ground shaking, soil failures, surface fault ruptures, or tsunamis. However, only ground shaking and soil conditions are explicitly considered. The commentary indicates that other hazards can be addressed through planning and site selection. This may lead structural engineers to assume that tsunamis are not critical and would not generate a significant loading event on structures.

2. CANADIAN TSUNAMI HAZARD

Given its geographical location and its proximity to highly active seismic areas, Canada remains susceptible to tsunamis, particularly along the west coast, where British Columbia meets the Pacific Ocean. Table 1 provides a list of major historical tsunami events that have affected the western coastlines of North America.

Table 1 Historical Tsunami Events along Canada's Coastlines

Date	Location	Maximum Run-up (m)
Nov. 4, 1994	Southern Alaska	7.6
Feb.4 1965	Western Alaska	10.7
Mar. 28, 1964	Gulf of Alaska	67.1
Mar. 9, 1957	Central Alaska	22.8
June 23, 1946	British Columbia	30
Sept. 10 1899	Gulf of Alaska	60
Nov. 18, 1929	Grand Banks, Newfoundland	13
Jan. 26, 1700	Cascadia, British Columbia	

Several of the events in Table 1 indicate that the tsunami hazard for Canada is significant, particularly for the Pacific coast. The March 28, 1964 Tsunami, which was triggered by a large earthquake in Alaska, resulted in millions of dollars in damage in Port Alberni, British Columbia. On January 26, 1700 a thrust fault rupture along the Cascadia Fault generated an earthquake measuring 9.0 on the Richter scale. This event triggered a tsunami wave that crossed the Pacific Ocean. According to oral traditions of First Nations, the tsunami completely destroyed the village of Pachena Bay situated on the west coast of Vancouver Island. There were no survivors. Given the presence of the Cascadia Fault and the Pacific "Rim of Fire", western Canada remains susceptible to tsunami events. To a lesser extent, the east coast of Canada, which borders the Atlantic Ocean, can also be affected, though not as often as the west coast, by tsunamis. On November 18, 1929, a 7.2 magnitude earthquake struck approximately 250 km south of Newfoundland, along the

southern edge of the Grand Banks, causing a large submarine landslide. In turn, a tsunami was generated, which hit the Burin Peninsula of Newfoundland, claiming 29 lives. This event represents the largest documented human loss in Canada linked to an earthquake. Note though, the tsunami was entirely responsible for the fatalities.

To understand the threat to western Canada, it is important to understand the geological features off the coast of British Columbia. From northern Vancouver Island to northern California, the Cascadia subduction zone marks the boundary between the smaller offshore Juan de Fuca Plate that is sliding under the much larger North American Plate. The Cascadia subduction zone has the potential to generate very large earthquakes, with magnitude 9.0 or greater, if the fault ruptures over its entire area. The January 26, 1700, Cascadia earthquake produced a fault rupture with a length of 1000 km. This type of event is similar to the 2004 Indian Ocean Earthquake, were the fault ruptured along an estimated length of 1300 km. Interestingly, both subduction zones run predominantly in a north-south direction, thus having the potential to trigger major tsunamis in the east-west direction. For Cascadia, this means that tsunami waves would propagate towards Vancouver Island. Popular belief suggests that major nearby cities, including Vancouver, Victoria, Seattle, and Portland, which are located on inland waterways rather than on the coast, would be sheltered from the full brunt of a tsunami wave. Meanwhile, numerical modeling has shown that tsunami waves would travel around Vancouver Island through diffraction and impact Victoria and Vancouver significantly (Xie *et al.*, 2007). This is consistent with observations following the 2004 Indian Ocean Tsunami, particularly on the west coast of Sri Lanka which was devastated by the tsunami as a result of wave propagation and diffraction around the island. Therefore, a megathrust earthquake along the Cascadia subduction zone has the potential to generate a major tsunami which would travel into the Juan de Fuca Strait, affecting communities along its shores.

Understanding the tsunami hazard is a major challenge in the design of near-shoreline structures. However, hazard maps, which would provide inundation depths and velocities for design in the case of a tsunami with a given magnitude and a given return period, are currently not available. At present, numerical modeling is employed to provide expected inundation depths for a given earthquake. Xie *et al.* (2007) conducted numerical modeling of tsunamis generated from a Cascadia Fault earthquake to assess the potential tsunami risk for western Canada. A magnitude 9.0 earthquake, similar to the event of 1700, was assumed in their model. The numerical model TSUNAMI N2 was employed. The model estimated a maximum wave run-up of 25 m along the western shore of Vancouver Island, with an estimated arrival time for the first wave of 1 hour and 20 minutes.

3. DESIGN CODES

Design codes in North America, which specifically address tsunami loading, are scarce. The City and County of Honolulu Building Code (CCH, 2000) and the Federal Emergency Management Agency Coastal Construction Manual (FEMA 55, 2003) are two documents that provide some guidance to engineers. The forces explicitly cited for a tsunami event

include buoyant forces, hydrostatic forces, hydrodynamic forces, debris impact forces, and surge or wave breaking forces. There are significant differences between the two documents. CCH determines surge forces generated by a tsunami bore-type wave, specifically for wall-type structural components. FEMA, on the other hand, considers wave breaking, which is typical of coastal floods and storm events. The FEMA document does not specifically address tsunami bores, which possess characteristics similar to those experienced during the December 24, 2004 Indian Ocean Tsunami. The other significant difference lies in the estimation of the flow velocity used in estimating the drag force. In CCH, the bore velocity is estimated to equal the depth of water at the building. FEMA, on the other hand, provides a significantly higher velocity in the area near the shoreline during a tsunami event. The flow velocity is estimated as $2\sqrt{gd_s}$, where d_s is the design flood depth. The consequence is larger drag forces in comparison to the estimates given by CCH. Only FEMA provides load combinations for the given force components; however, these combinations are explicitly formulated for flood scenarios and include wave breaking forces. Nistor *et al.* (2008) proposed loading combinations (Figure 1) that specifically consider a tsunami event including the effects of a bore-type wave.

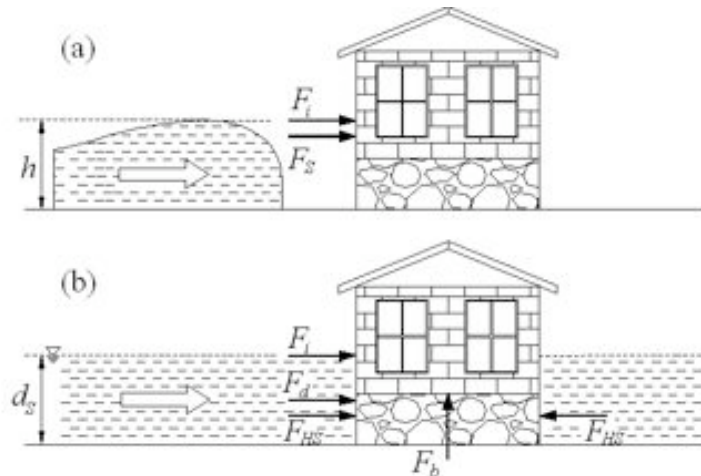


Figure 1 Proposed Tsunami Loading Combinations: a) Initial Impact; b) Post Impact (Nistor *et al.* 2008)

The first loading combination (Initial Impact) considers surge and debris impact forces as the main lateral load components. This represents the first impact of the tsunami bore. The second scenario (Post Impact) includes debris impact, hydrodynamic, and hydrostatic forces as the lateral loads. Note that the net hydrostatic forces typically provide an insignificant lateral load to the structure as a whole. However, the hydrostatic force may be more important in the evaluation of loads on an individual wall element. In addition to the lateral loads, a buoyant force component is included in the post impact event. This force can cause stability problems, including a reduction in the sliding and overturning resistance of a structure. Furthermore, consideration should be given to the rapid rising water level within a structure that has been flooded. This phenomenon can result in significant uplift forces on flooring elements (Ghobarah *et al.*, 2006).

The tsunami load can be combined with other loads and implemented in building codes. From the National Building Code of Canada (NBCC 2005) perspective, load cases following the philosophy of earthquake loading are suggested as a preliminary framework. A tsunami load is considered to be an extreme event leading to the following three load cases (Eqn. 1.1). The first load case considers Tsunami (T) and Dead (D) loads only. The second load case includes companion loads, including Live (L) and Snow (S) loads. The third case should only be considered if early warning systems provide sufficient warning to allow occupants to exit buildings safely.

$$\begin{aligned}
 &1.0T + 1.0D \\
 &1.0T + 1.0D + 0.5L + 0.25S \\
 &1.0T + 1.0D + 0.25S
 \end{aligned}
 \tag{1.1}$$

Note that in the case of the Cascadia subduction zone along the western coastline of British Columbia, damage to structures may initial occur due to the triggering earthquake before the tsunami-induced loading arrives. In such cases, engineers should consider the effects of the tsunami load on softened or damaged structures.

4. STRUCTURAL ANALYSIS

A simple, 10-storey ductile reinforced concrete moment resisting frame structure is analyzed for tsunami and seismic loads for the Vancouver area. The tsunami inundation level is assumed to be 5 m. The seismic weight is approximately 4400 kN per floor and the storey heights are 3.65 m. Figure 2 shows a plan view of the structure, while Table 2 provides the force components considered in calculating the tsunami loading.

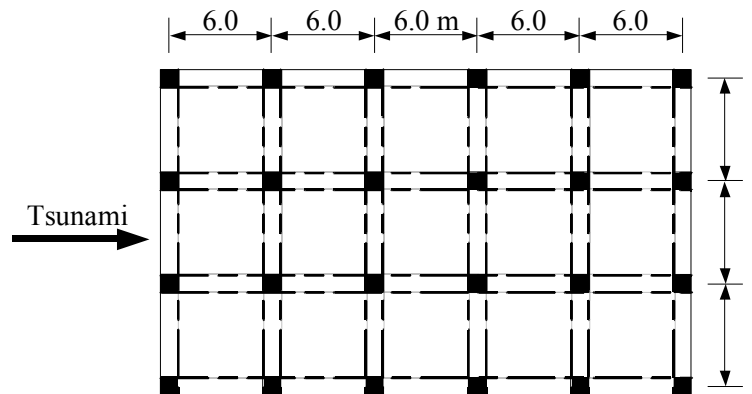


Figure 2 Building Plan Layout (Palermo *et al.*, 2007)

Table 2. Force Components for Tsunami Loading

Flow Velocity u	Surge F_s	Hydrodynamic F_d	Debris Impact F_i
$2\sqrt{gd_s}$	$4.5\rho gh^2b$	$\frac{\rho C_D Au^2}{2}$	$m\frac{u}{\Delta t}$

The calculated elastic base shear for the building under seismic effects is approximately 13720 kN, and considering ductility is 2020 kN. A 5 m tsunami level would induce an approximate base shear of 20360 kN due to the surge force during the initial impact and 11300 kN during the post impact caused by the drag of the tsunami flow around the structure. If the velocity component is assumed to be equal to the tsunami inundation level as assumed by CCH, the post impact phase would generate a base shear of 1730 kN. While this example is intended to provide an understanding of the tsunami forces imposed on structures, it also highlights the importance of properly quantifying the tsunami force components. The surge force is estimated as nine times the hydrostatic force; however, this has not been widely accepted in the literature. Furthermore, the velocity generated by the tsunami bore varies significantly, which affects the magnitude of the drag forces. This example also assumes that all non-structural exterior elements remain intact. It is highly probable that the first impact of the tsunami wave damages the exterior non-structural components, reducing the lateral load that is transferred to the structure. As such, the non-structural components act as a fuse for the lateral load resisting system. [Note: The debris impact loading according to FEMA and CCH is negligible in the calculation of the global base shear and has therefore been omitted.]

5. EXPERIMENTAL PROGRAM

Considerable disagreement and uncertainty exists in the literature regarding the force components and the tsunami-induced bore velocity. Particularly, the surge force is of question. To address and better understand the forces generated during a tsunami event, an exhaustive and comprehensive experimental program was conducted by the University of Ottawa in cooperation with the Canadian Hydraulics Centre in Ottawa, Canada.

The testing was carried out in a high discharge flume measuring 10.0 m in length, 2.7 m in width, and 1.4 m in height. The flume is serviced by pumps that can deliver a variable discharge flow up to 1.7 m³/s. For this experimental program, the flume was partitioned to create a testing zone 1.3 m wide and 7.3 m long. A hinged gate was designed and installed near the upstream section of the flume. In the closed position, the gate could impound a specified depth of water (impoundment depth). The hinging mechanism of the gate permitted a rapid opening, allowing a turbulent hydraulic bore to travel down the flume. Figure 3 provides a schematic of the testing facility.

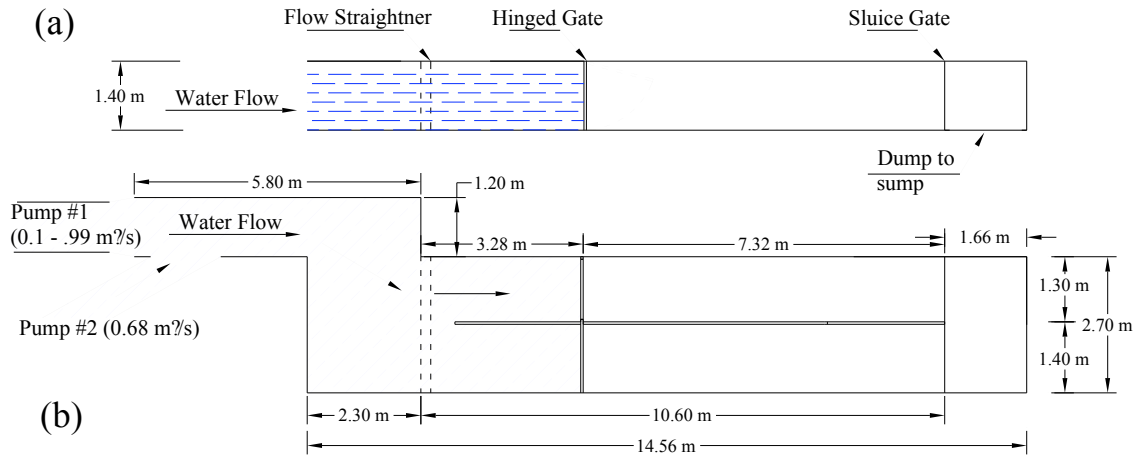


Figure 3 Wave Flume Setup: a) Elevation View; b) Plan View (Nouri 2008)

Forces created by the hydraulic bore were measured for two structural components: square/diamond, and circular sections. Figure 4 is a photo of the structural elements used for the experimental program of this study. The circular section was made of PVC pipe and measured 0.32 m in diameter, whereas the square/diamond section was assembled from acrylic Plexiglas and had a cross section of 0.2 m x 0.2 m. The circular section was mounted onto a 6-axis dynamometer, allowing base shears and moments to be recorded directly. In addition, nine pressure transducers were placed flush along a vertical column on the circular section. This was used to establish the time-history pressure profiles of the loading. The square/diamond section, on the other hand, was instrumented with five pressure transducers, which recorded local forces. The flume was equipped with ADV sensors and wave gauges to record flow velocities and depths, respectively.

The testing program consisted of 11 test series, and included varying upstream impoundment depths, debris weights, and constrictions. Additional information on the testing program is available in Nouri (2008). For brevity, a sample of the experimental testing will be discussed herein.



Figure 4 Circular and Square/Diamond Structural Components

6. EXPERIMENTAL RESULTS

Of particular interest to structural engineers are the force components expected during a tsunami event. Figure 5 provides the global force-time histories of the base shears experienced by the circular section.

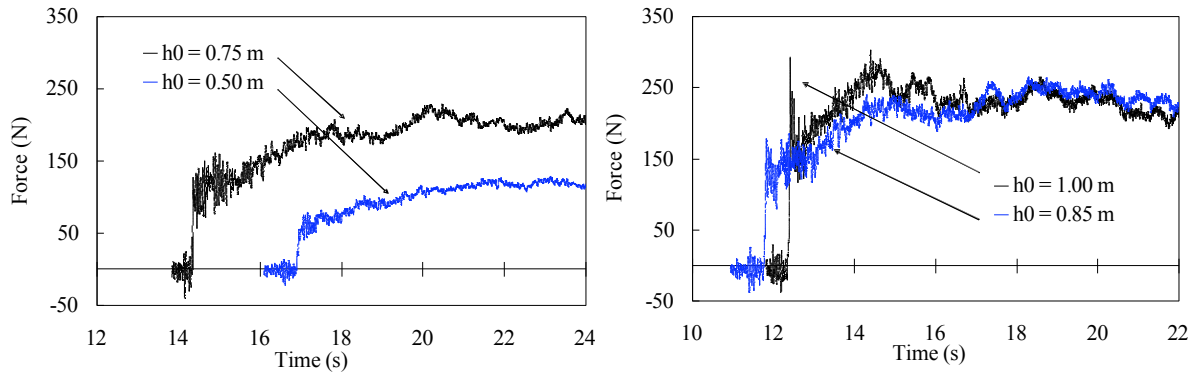


Figure 5 Force-Time History for Circular Section (Nouri 2008)

Figure 5 provides the base shears for impoundment depths of 0.5 m, 0.75 m, 0.85 m, and 1.0 m. The first abrupt rise in force is caused by the initial impact (surge force) of the hydraulic bore on the structure. With increasing upstream water depth, the surge force increases. This increase is partly due to the larger impoundment depth and the increase in bore front slope with increasing impoundment depth. Immediately following the initial impact, there is a drop in the base shear. For the 0.75 m, 0.85 m, and 1.0 m impoundment depths, the reduction in force ranges between 55% and 60% of the initial impacting force. For the 0.50 m impoundment depth, the drop in the base shear force is approximately 30% of the initial magnitude. This drop is followed by a gradual increase caused by the run-up of the hydraulic bore. In all cases, the run-up force was equal to or greater than the initial impacting load. The run-up is followed by a semi-steady state of flow characterizing the drag force. Excluding the 1.0 m impoundment depth, the drag force represented the largest force component in the loading history. Figure 6 shows the individual force components for a 1.0 m impoundment depth, along with the corresponding bore height.

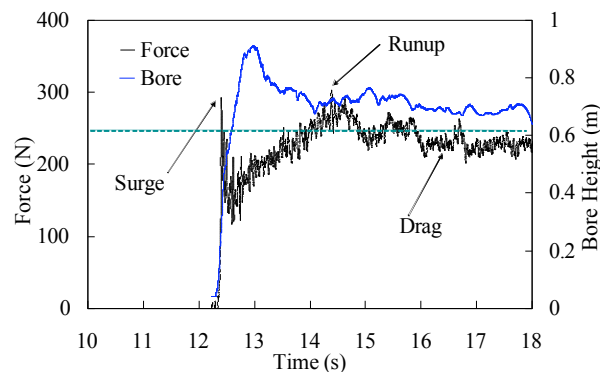


Figure 6 Time-History of Force Components on Circular Section

Figure 7 (a) provides the pressure-time history for the circular section along the height while Figure 7 (b) provides the pressure distribution corresponding to the individual force components.

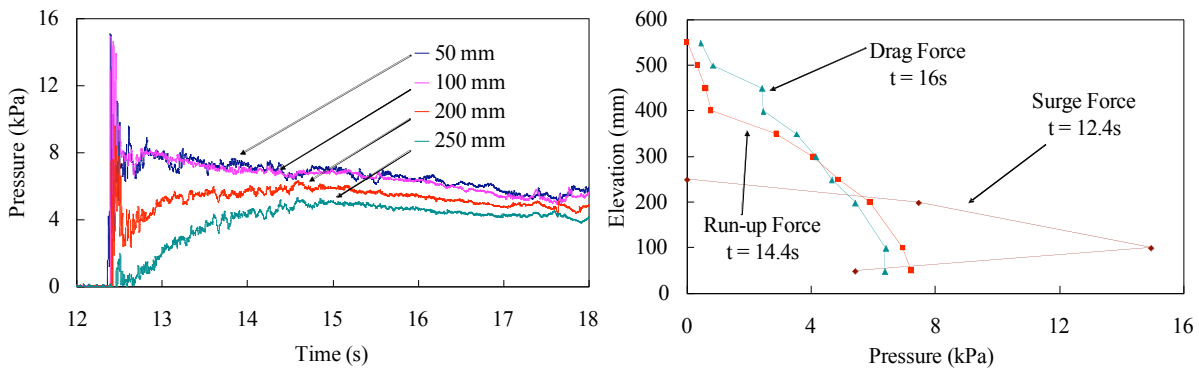


Figure 7 Pressures: a) Time-History Along Height of Column; b) Distribution Corresponding to Forces

Pressures are shown at 50 mm, 100 mm, 200 mm, and 250 mm from the base of the circular section. At the instant of the initial impact of the hydraulic bore, the pressure distribution is approximately triangular, as indicated by the surge force component at 12.4 s. The pressure distributions become increasingly constant at the point of the run-up and drag force components, shown at 14.4 s and 16 s, respectively. Variations in the velocity along the height of the bore are partly responsible for variations in pressure for the drag force component.

To simulate debris impact loading, a wooden log, 445 mm long and with a 90 mm x 90 mm cross-section, was used. Figure 8 illustrates the effect of debris on the force-time history for the circular section with impoundment depths of 1.0 m and 0.75 m. The debris caused a significant increase in the base shear recorded by the dynamometer mounted at the base of the circular section. A spike is evident a short time after the initial impact of the hydraulic bore. For the 1.0 m impoundment depth, an increase in the base shear force of 695 N occurred over a rise time of 0.0075 s, whereas the base shear force increased by 430 N over a period of 0.008 s for the 0.75 m impoundment. The results shown for the 0.75 m impoundment demonstrate a second peak a short time after the initial debris impact. This phenomenon was caused by a “bounce back” effect of the wooden log causing a subsequent impact. The second peak was always smaller in magnitude; however, the rise time was similar to the first debris impact. This “bounce back” effect was observed for other impoundment depths as well.

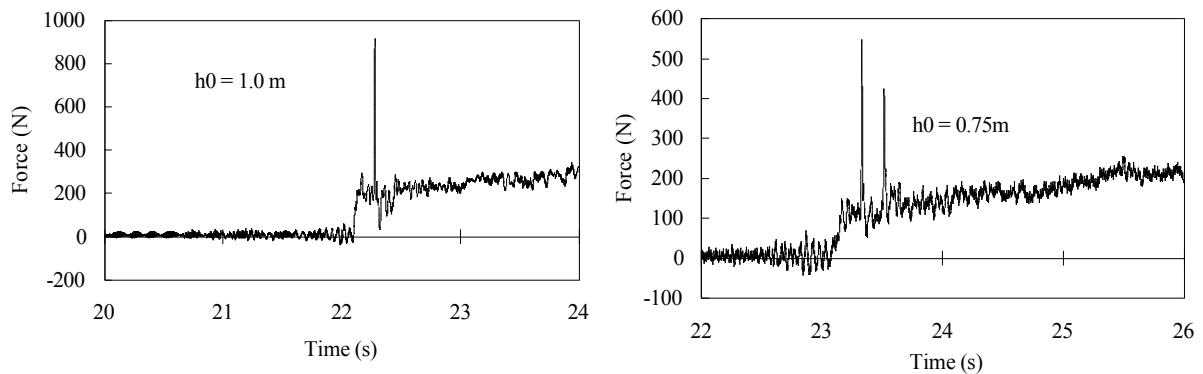


Figure 8 Debris Impact Loading on Circular Section

7. CONCLUSIONS

This paper provides background information regarding the tsunami threat to Canada and, in particular, the west coast. In addition, results from an experimental program, aimed at better understanding the forces generated by a turbulent hydraulic bore, are presented. The following conclusions are drawn from these experiences:

1. Tsunami-induced loading should be considered for near-shoreline structures located in tsunami-prone areas.
2. More guidance is required for structural engineers in order to estimate tsunami loads on structures.
3. Improved estimates of bore velocities are required to provide more accurate drag and debris impact forces.
4. Based on the impoundment depths investigated, the experimental results indicate that the surge force does not significantly overshoot the drag force as indicated by current codes.
5. Pressure readings of the circular section indicate that the initial bore impact causes an approximate triangular pressure distribution along the height of the section.
6. Debris impacting structures can produce a “bounce back” effect, causing a second lower amplitude impact.

REFERENCES

Canadian Commission on Building and Fire Codes (2005). "National Building Code of Canada (NBCC)," National Research Council of Canada, Ottawa, Canada.

Department of Planning and Permitting of Honolulu Hawaii (2000). "City and County of Honolulu Building Code," Chapter 16, Article 11.

Federal Emergency Management Agency (2003). "Coastal Construction Manual," FEMA 55, Jessup, MD.

Ghobarah, A., Saatcioglu, M. and Nistor, I., (2006). The impact of 26 December 2004 earthquake and tsunami on structures and infrastructure, *J. Engineering Structures*, Elsevier, Vol. 28, 312-326.

Nistor, I., Palermo, D. Nouri, Y., Murty, T., and Saatcioglu, M. (2008), Tsunami forces on structures, Chapter 11 in "*Handbook of Coastal and Ocean Engineering*", Editors: Dr. Kim Young (UCLA), World Scientific, Singapore (in press).

Nouri, Y. (2008). "The Impact of Hydraulic Bores and Debris on Free Standing Structures," M.A.Sc. Thesis, Department of Civil Engineering, University of Ottawa, Ottawa, Canada.

Palermo, D., Nistor, I., Nouri, Y., and Cornett, A. (2007). "Tsunami-Induced Impact and Hydrodynamic Loading of Near-Shoreline Structures." *PROTECT 2007* (First International Workshop of Performance, Protection, and Strengthening of Structures under Extreme Loading), Whistler, Canada.

Xie, J., Nistor, I., and Murty, T. (2007). "Tsunami Risk for Western Canada and Numerical Modeling of the Cascadia Fault Tsunami," *18th Canadian Hydrotechnical Conference*, Winnipeg, Canada.

MINIMIZING COMPUTATIONAL ERRORS OF TSUNAMI WAVE-RAY AND TRAVEL TIME

Andrei G. Marchuk

Institute of Computational Mathematics and Mathematical Geophysics,
Siberian Division, Russian Academy of Sciences, Novosibirsk, RUSSIA
mag@omzg.ssc.ru

ABSTRACT

There are many methods for computing tsunami kinematics directly and inversely. The direct detection of waves in the deep ocean makes it possible to establish tsunami source characteristics and origin. Thus, accuracy of computational methods is very important in obtaining reliable results. In a non-homogeneous medium where tsunami wave propagation velocity varies, it is not very easy to determine a wave-ray that connects two given points along a path. The present study proposes modification in the methodology of determining tsunami travel-times and of wave-ray paths. An approximate ray trace path can be developed from a source origin point to any other point on a computational grid by solving directly the problem - and thus obtain the tsunami travel-times. The initial ray approximation can be optimized with the use of an algorithm that calculates all potential variations and applies corrections to travel-time values. Such an algorithm was tested in an area with model bathymetry and compared with a non-optimized method. The latter exceeded the optimized method by one minute of travel-time for every hour of tsunami propagation time.

1. Travel-time computations in non-homogeneous areas.

Numerical modeling of tsunami wave propagation can provide better understanding of the phenomenon. Tsunami wave propagation and travel times can be calculated for different time intervals (isochrones) and various numerical methods have been developed [1]. For areas with complicated geomorphology and bathymetry (islands and narrow straits), travel-time computations based on methods that use Huygen's principle are more effective than others [2]. The basic premise in using this principle requires that all points of the source area where the tsunami wave was generated be sources of omni-directional wave energy radiation. The algorithm for such computation searches through all adjacent grid-points to the generated wave front and calculates the minimum of all tsunami travel time interval through these points.

The sum total of all travel-times from the source point to a final point is the minimum for all possible wave travel paths. Rectangular computational grids with known ocean depth values are used normally for travel-times calculations from the source region to all terminal points. Figure 1 shows a grid fragment of such a computational area. The small black squares designate points on the grid, where the wave from the initial tsunami source has arrived and the tsunami travel-times to these grid-points are known.

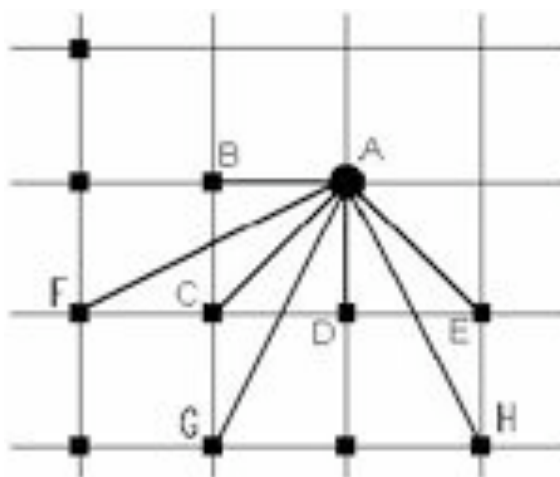


Fig. 1. The scheme of travel-time determination using Huygens's principle

We need to find the travel-time from the source up to the point A. Relative to the point A, the neighboring points, where the travel-times are known, there will be the points B, C, D, E, F, G and H. Let the travel-times up to them be equal to T_B , T_C , T_D , T_E , T_F , T_G and T_H respectively. Between the adjacent grid-points the depth is varying linearly. To determine the tsunami travel-time, we take the distance between two neighboring grid-points L , and a depth value varying from H_1 up to H_2 . The angle of bottom declination is the auxiliary value α , which can be designated as

$$\operatorname{tg}(\alpha) = (H_2 - H_1) / L$$

Then the tsunami travel-time for that time increment can be expressed as:

$$\begin{aligned}
 T &= \int_0^L \frac{dl}{\sqrt{g \cdot (H_1 + l \cdot \operatorname{tg} \alpha)}} = \frac{1}{\sqrt{g \cdot \operatorname{tg} \alpha}} \int_0^L \left(l + \frac{H_1}{\operatorname{tg} \alpha} \right)^{-1/2} d \left(l + \frac{H_1}{\operatorname{tg} \alpha} \right) = \\
 &= \frac{2}{\sqrt{g \cdot \operatorname{tg} \alpha}} \left(l + \frac{H_1}{\operatorname{tg} \alpha} \right)^{1/2} \Big|_0^L = \frac{2}{\sqrt{g \cdot \operatorname{tg} \alpha}} \cdot \frac{\sqrt{H_2} - \sqrt{H_1}}{\sqrt{\operatorname{tg} \alpha}} = \\
 &= \frac{2}{\sqrt{g \cdot \operatorname{tg} \alpha}} \cdot \frac{H_2 - H_1}{\sqrt{H_2} + \sqrt{H_1}} = \frac{2L}{\sqrt{gH_2} + \sqrt{gH_1}}.
 \end{aligned} \tag{5}$$

Therefore, the tsunami travel-time between the neighboring grid-points is equal to a distance between them divided by the arithmetically averaged velocity of the tsunami at these grid-points. Thus, in order to find the travel-time from the source up to a point **A** (fig. 1), it is necessary to find a minimum of seven time values

$$\begin{aligned}
 T_1 &= T_B + \frac{2 \cdot \Delta x}{\sqrt{gH_B} + \sqrt{gH_A}}, & T_2 &= T_C + \frac{2 \cdot \sqrt{(\Delta x)^2 + (\Delta y)^2}}{\sqrt{gH_C} + \sqrt{gH_A}}, \\
 T_3 &= T_D + \frac{2 \cdot \Delta y}{\sqrt{gH_D} + \sqrt{gH_A}}, & T_4 &= T_E + \frac{2 \cdot \sqrt{(\Delta x)^2 + (\Delta y)^2}}{\sqrt{gH_E} + \sqrt{gH_A}}, \\
 T_5 &= T_F + \frac{2 \cdot \sqrt{(2\Delta x)^2 + (\Delta y)^2}}{\sqrt{gH_F} + \sqrt{gH_A}}, & T_6 &= T_G + \frac{2 \cdot \sqrt{(\Delta x)^2 + (2\Delta y)^2}}{\sqrt{gH_G} + \sqrt{gH_A}}, \\
 T_7 &= T_H + \frac{2 \cdot \sqrt{(\Delta x)^2 + (2\Delta y)^2}}{\sqrt{gH_H} + \sqrt{gH_A}},
 \end{aligned} \tag{6}$$

Where $\Delta \mathbf{x}$, $\Delta \mathbf{y}$ - steps of a grid in horizontal and vertical directions and H_A , H_B , H_C , H_E , H_F , H_G , H_H - the depth values at the corresponding points. Minimum of values T_i ($i=1, 2, 3, 4, 5, 6, 7$) will give us the tsunami travel-time from the source up to a point **A**. In such a way it is possible to find point by point the travel-times to all the points of a computational grid.

As for the neighboring grid-points, the following can be stated. The simplest one is the eight-dot template (Fig. 2).

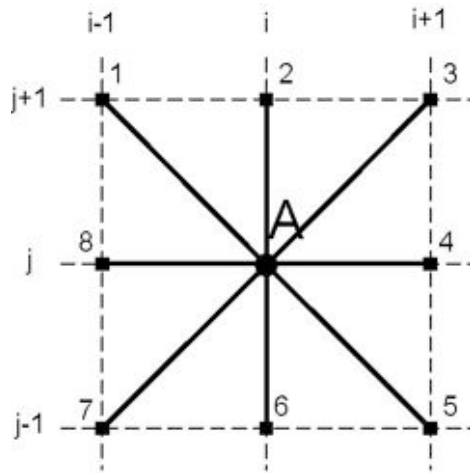


Fig. 2. The eight-dot template for computation of tsunami travel-times.

In such a template the following eight grid-points: $(i-1, j+1)$, $(i, j+1)$, $(i+1, j+1)$, $(i+1, j)$, $(i+1, j-1)$, $(i, j-1)$, $(i-1, j-1)$, $(i-1, j)$ will be the neighboring ones to point A with the grid coordinates (i, j) . The travel-times from each of them to the central point are calculated along eight straight segments. Therefore, this template is sometimes called the eight-radial (eight-dot). However, this template is too simplified and, as a result, the wave front computations from a point source using this template give above the bottom of constant depth an octagonal front line instead of a circle.

More precise results can be obtained if for computations use a sixteen-dot (sixteen-radial) template (Figure 3).

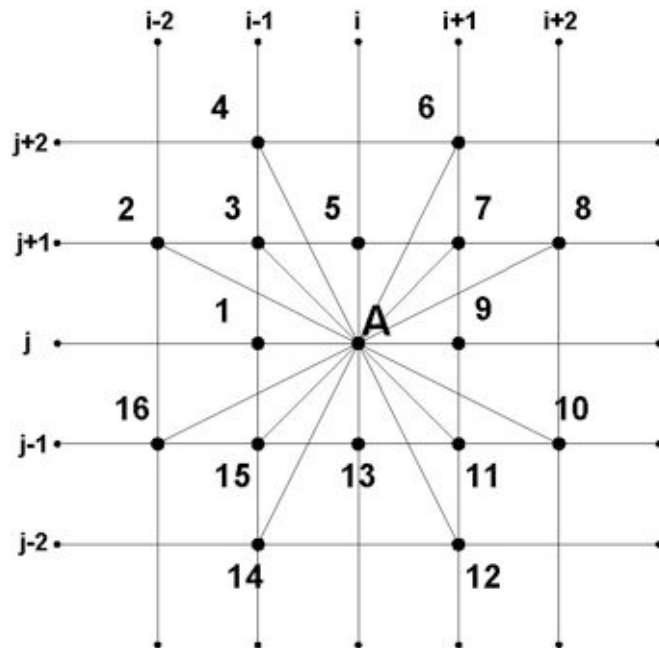


Fig. 3. The sixteen-dot template for tsunami travel-time calculations on a rectangular computational grid.

In this template, the neighbors to the point A, that has the grid coordinates (i, j) , are the grid-points

whose indices differ from the grid coordinates of the point **A** not only by one, but also by some grid-points whose coordinates differ by two (see Figure 3). In this case, if at any of these 16 points the tsunami travel-time is already known, it is possible to find the wave travel-time to point **A** (at the center of the template).

2. Method for determination of tsunami wave rays in areas with variable depth.

However, the above-described method for travel-time computations does not give directly the traces of the wave rays. In order to determine wave-ray traces with this method, the following algorithm is proposed. Since it is necessary to find the path of the wave ray between two given points in the computational domain, the first step is to calculate travel-times from one of these points to all the other grid points of the computational domain. During the process of travel-time determination at the point (i, j) the grid coordinates of the neighboring point are stored in the computer memory. After completing the computations, two matrices $n_x(i, j)$ and $n_y(i, j)$ with the dimensions of the whole computational area will be filled. The entries of the first array are the horizontal coordinates and in the second array there are vertical grid coordinates of those points (fig. 4). With the help of these two arrays it is very easy to reconstruct a ray trace from an arbitrary grid-point to the source point. Reconstruction starts at a receiving point.

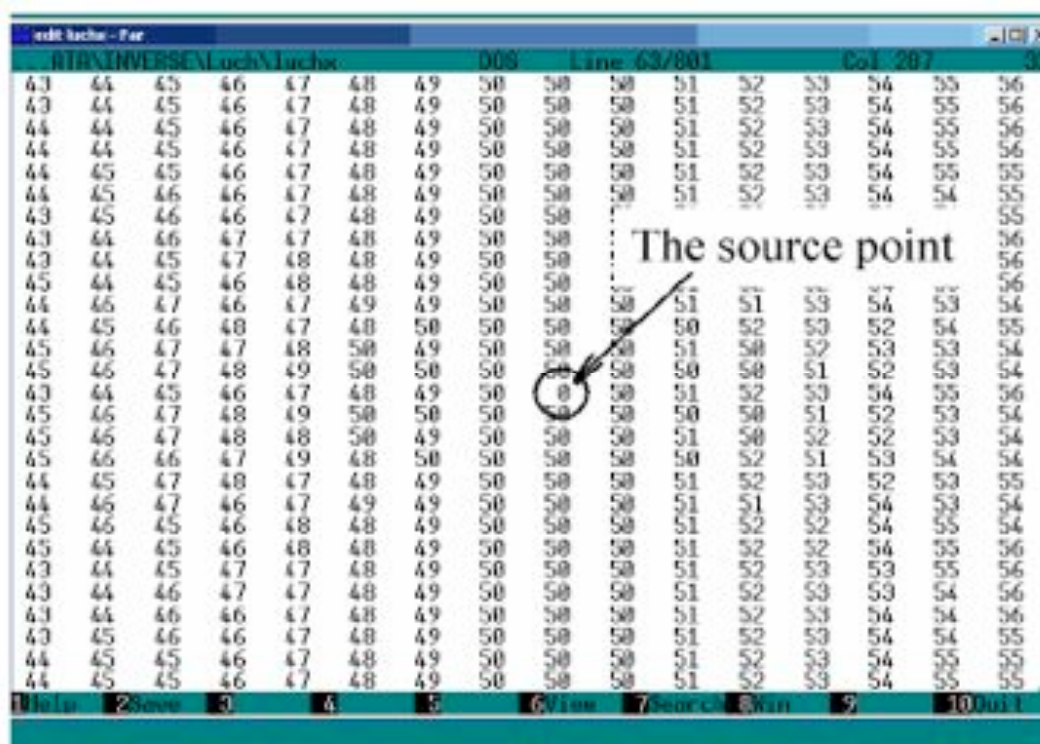


Fig. 4. Fragment of $n_x(i, j)$ array. The source is located at the grid-point (50,50).

Figures 5-6 show an example of the ray reconstruction process in a small sub-section of the entire computational domain. The grid coordinates are indicated at the top and at the left edges of the

Figure. For example, if there is a need to build a wave ray between the points with grid coordinates (10, 10) and (16, 11) (fig.5), the first step will be to calculate travel times in the whole computational domain from the source, which is at point (10, 10). For some of the grid-points in Figure 5 in parentheses we give pairs of numbers from those two arrays $n_x(i, j)$ and $n_y(i, j)$, which were obtained during travel-time computations.

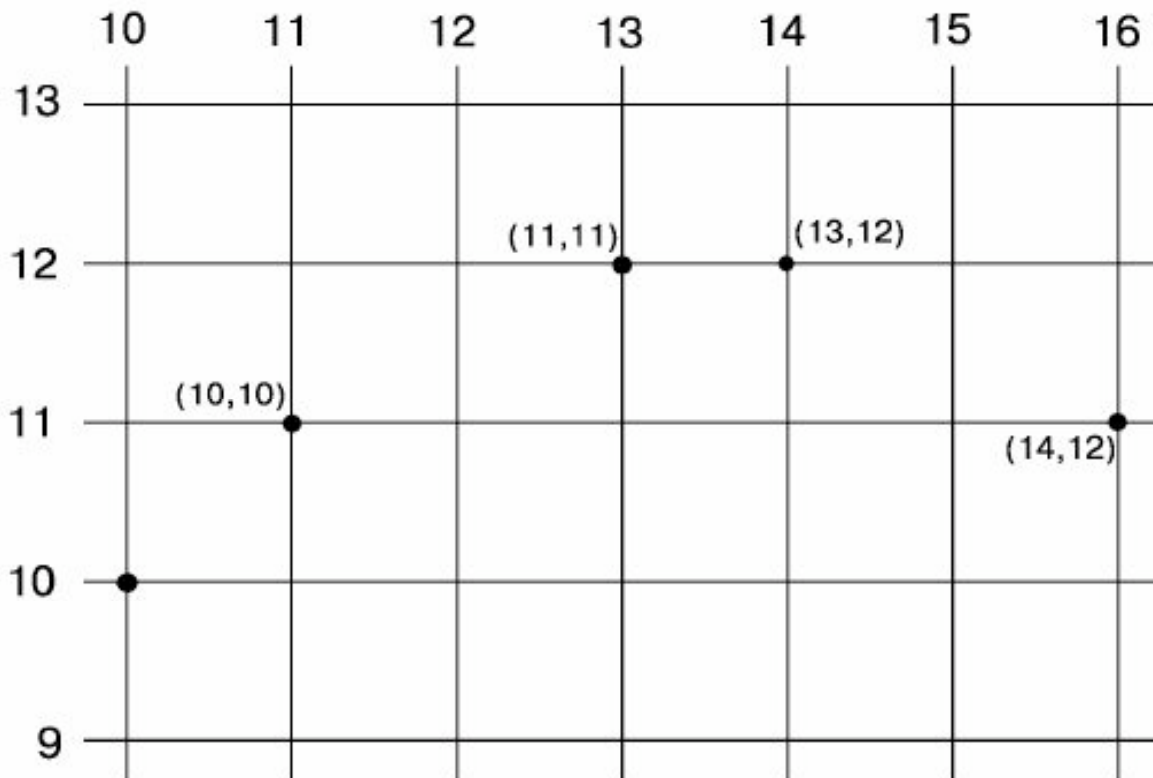


Fig. 5.

If the reconstruction starts at point (16, 11), the sequence of grid-points, which gives the quickest route for wave propagation from point (10, 10) to point (16, 11) can be easily determined. Conjunction of grid-points (16, 11), (14, 12), (13, 12), (11, 11), (10, 10) gives the tsunami wave ray (see fig. 6). If we draw a line through these points, then we will obtain an approximate ray trace connecting points (10, 10) and (16, 11). The wave rays determined by this method consist of segments of the rays of the template (“star”) (see Figures 2 and 3). When the 8-dot template (see Figure 2) is used, the segments of the defined ray can have only eight variants of direction. When using a 16-dot template, the number of variants increases to 16, which indicates that the approximation to the real wave ray path is significantly improved.

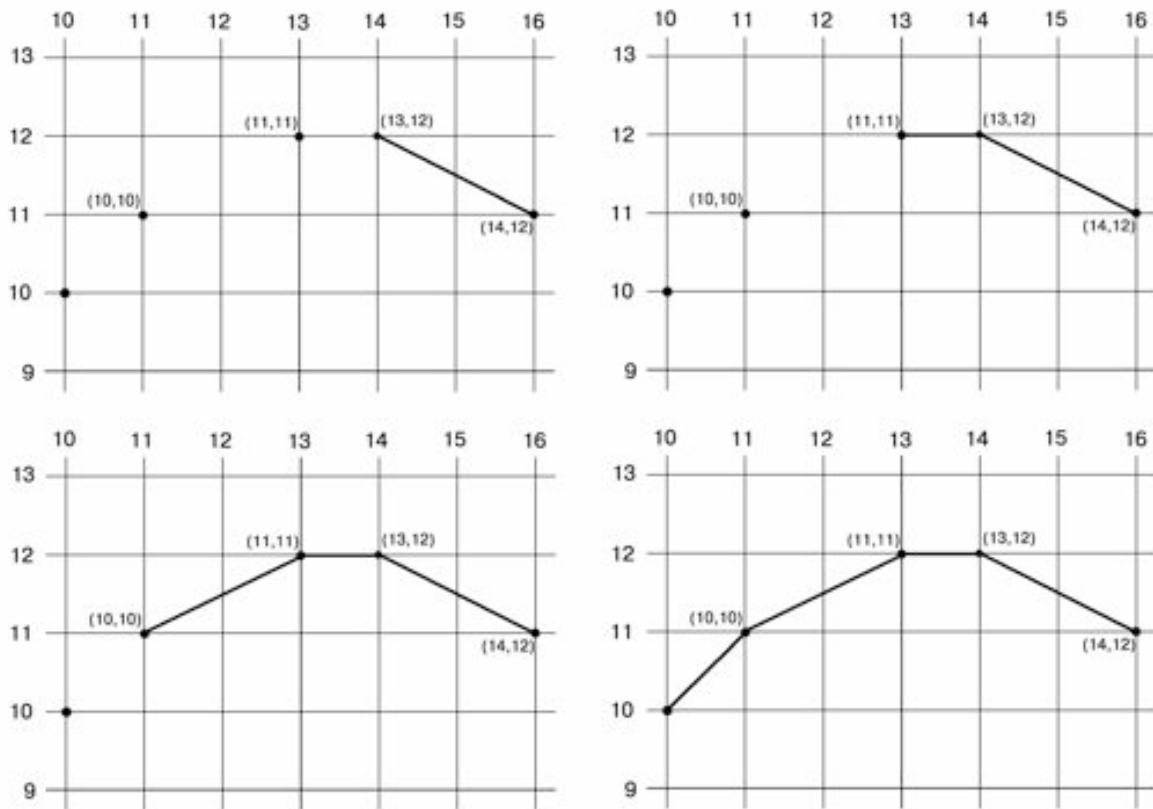


Fig. 6. The reconstruction of the ray trace between two points.

The main disadvantage of these wave-ray determination methods is the limited variety of directions of ray segments. For the 16-dot template this number is 16. Ray traces after this kind of computations are not smooth enough. Figures 7 and 8 show tsunami wave-rays for areas with actual bathymetry. In the Figure 7 the tsunami wave-rays connect the mouth of the Avacha harbor (Southern Kamchatka) and three other points of this area. One point is the Severo-Kurilsk village at the southern part of the area and the other two points are located on the Kamchatka shelf. The next figure (Fig. 8) shows the tsunami wave-ray traces in the eastern part of the Indian Ocean in areas of gradually varying depth (between Nicobar Islands and Sri Lanka) where the wave-rays look like straight lines.

3. Accuracy improvement of the tsunami travel-time computations

Also, a limited number of ray segment directions cause errors in the determination of the travel-time values at grid-points. These travel-time mismatches can be easily seen in the figure 9, where isolines for travel-time computations at an area with flat bottom are displayed. The dimension of computational area is 1,000x1,000 points with grid-steps equal to 1 km in both directions and ocean depth being 1,000 m. When the tsunami travel times are determined correctly, the shapes of isochrones must be circles. However, in actuality, instead of circles after the computations we have 16-angle polygons (fig. 9).

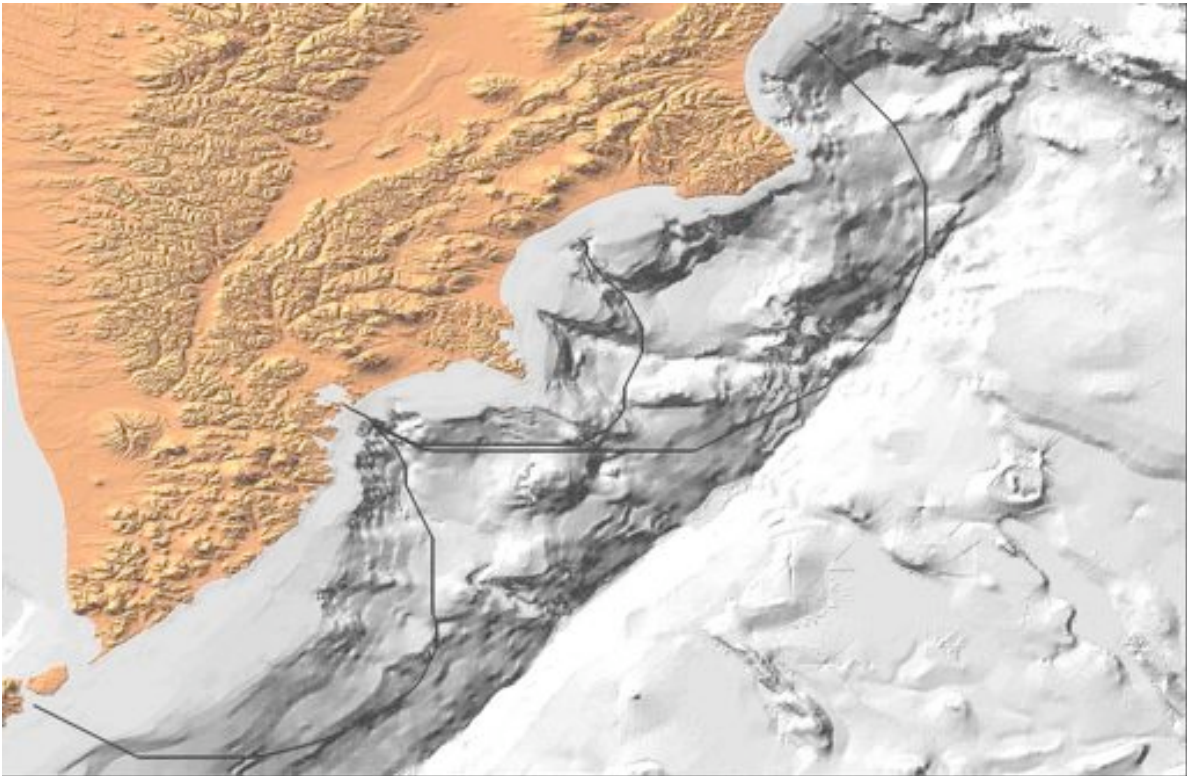


Fig. 7. The bottom topography and the wave rays near Kamchatka.

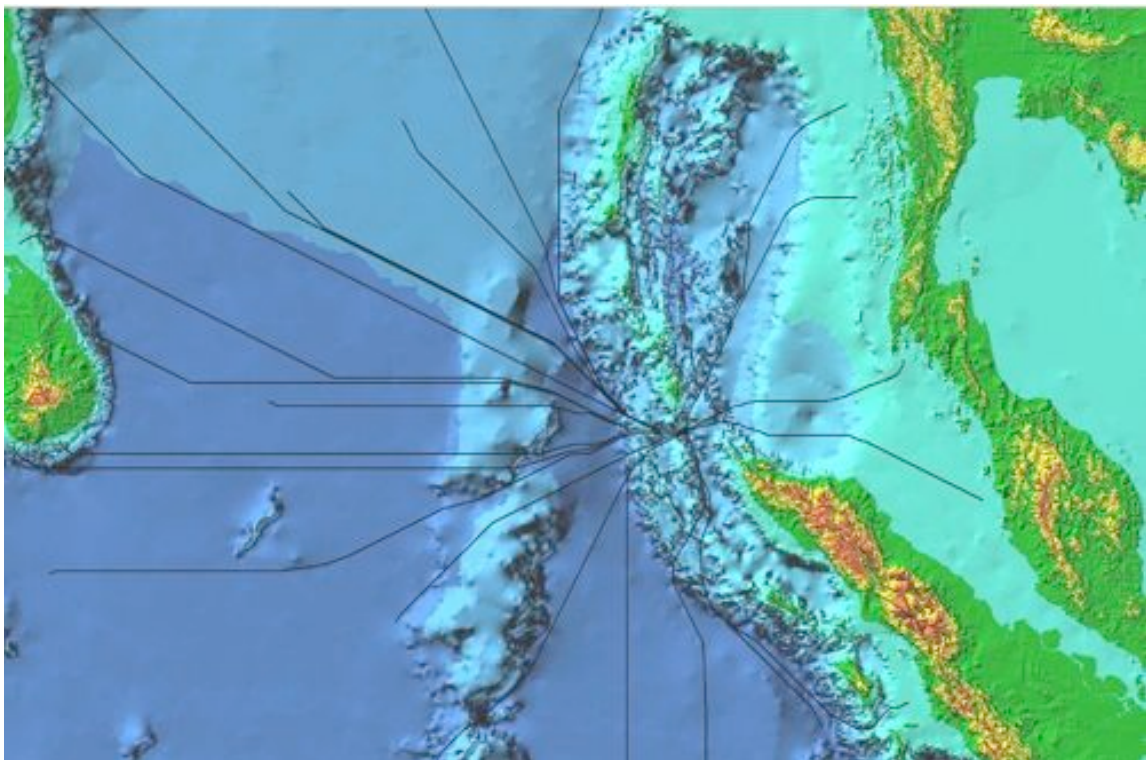


Fig. 8. The bottom topography and the wave rays in the eastern part of the Indian Ocean.

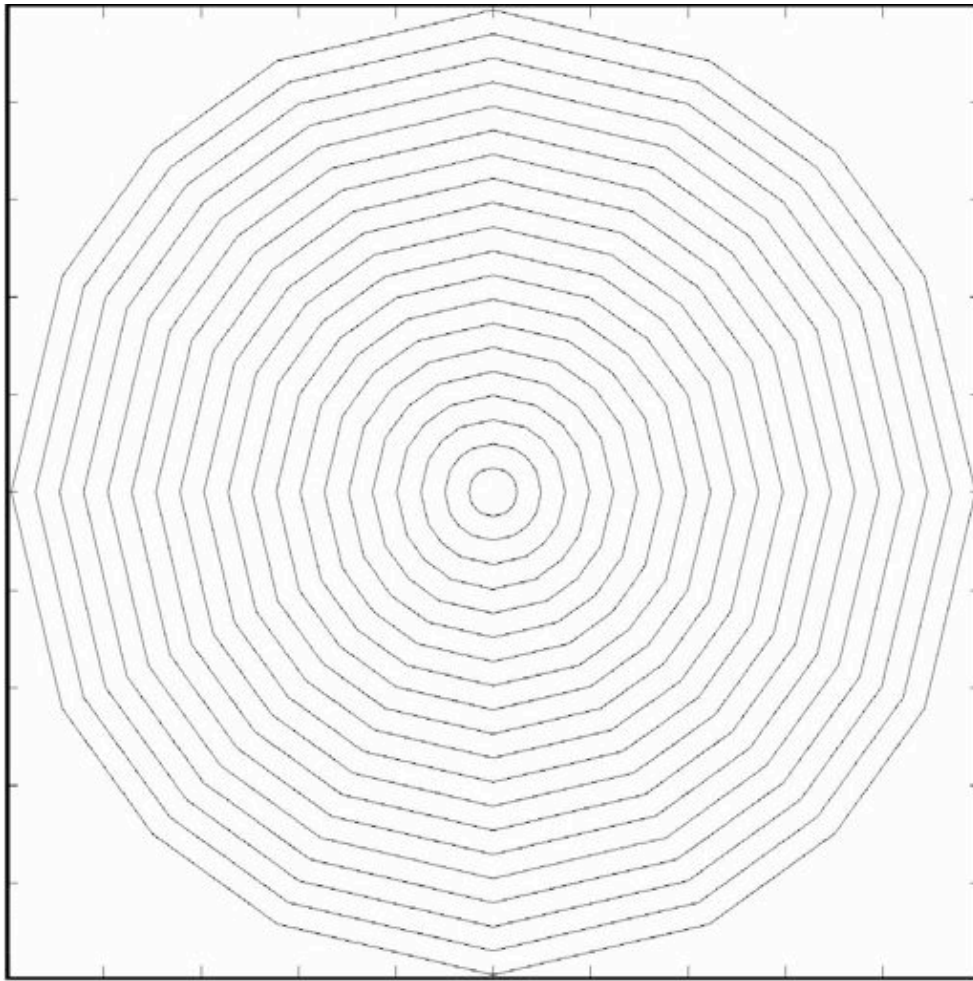


Fig. 9. The test isochrones computation in the area of constant depth using sixteen-dot template (area size 1,000x1,000, isochrones from 0 to 5,000 seconds with 250 sec steps).

One of the ways to improve the accuracy of approximation is to include more points to the calculation process. For example, it is possible to use a 32-dot template, but in this case the total number of arithmetic operations increases by two times. In addition, the long distances between some points of the template and its center (up to 3 grid-steps) will cause errors in resulting travel-times. The resulting approximation of the wave ray (as shown in the figure 6) consists in a number of straight segments. It is possible to improve significantly the approximation quality by using the technique of variations. Briefly, this means searching for new locations of points along the wave ray. These new points do not have to be grid-points. Within every grid-point included into the calculation the wave ray trace advances with very small incremental steps (1/10 of the grid) in different directions along the grid lines until a new location provides the shorter propagation time along the wave ray path.

To describe the optimization algorithm consideration is given to the small segment of a computational area (figure 10). During the travel-time calculation process, if line **SABCD** is designated to be the wave-ray trace between the source **S** and the target point **D**, the path of the ray

between the source point and any other grid-point can be restored. The procedure for obtaining more precise travel-time values by relocation of points **B**, **C** and **D** is as follows. During the computation process the algorithm will estimate the travel-time at a point **B**, then the correctional procedure is applied. The grid-point **A**, which is situated at the ray trace between points **S** and **B**, must be relocated along the horizontal and vertical axis within small step (about 1/10 of a grid-step). At every new position of this intermediate point A_1 a travel-time along the trace SA_1B will be calculated, based on the assumption that the depth between two neighboring grid-points varies linearly.

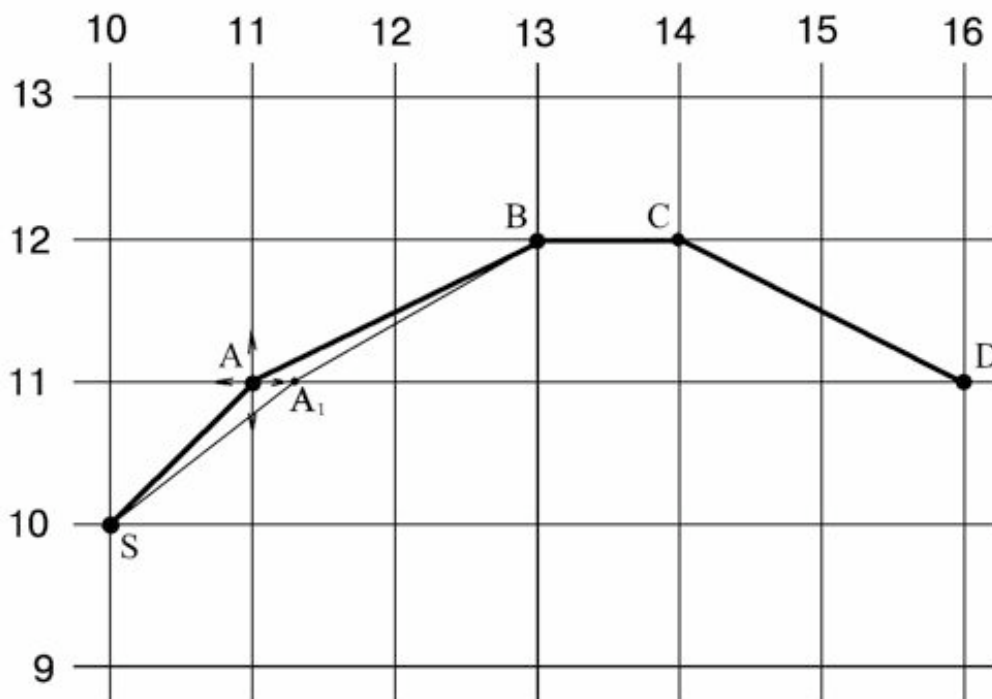


Fig. 10. The scheme of the ray-trace optimization procedure.

The minimum travel-time value will be accepted as the corrected travel-time at point **B**. It is of great importance that for further computations the corrected travel-time value at point **B** be used. When the general algorithm (based on the sixteen-dot template) gives the preliminary travel-time value at point **C**, then the correction procedure must be repeated again for another three grid-points (**A**, **B** and **C**). As a result, a new corrected value of travel-time at a point **C** will be defined. Such a correctional procedure will be applied to all grid-points along the ray path. Figure 11 shows the result of wave ray optimization with the ray trace indicated above the parabolic bottom slope. In this computational area the depth increases as a squared distance from the left boundary (Y axis). In the left part of the figure the ray is displayed before optimization and in the right part – after optimization. The optimized ray trace is much smoother than the initial one. The shape of optimized ray (right drawing in figure 11) shows a good correlation with the analytical solution, being the segment of a circle. As far as travel-times are concerned, such type of optimization can be applied to the process of travel-times computations. This procedure for a travel-time correction is presented schematically in figure 12.

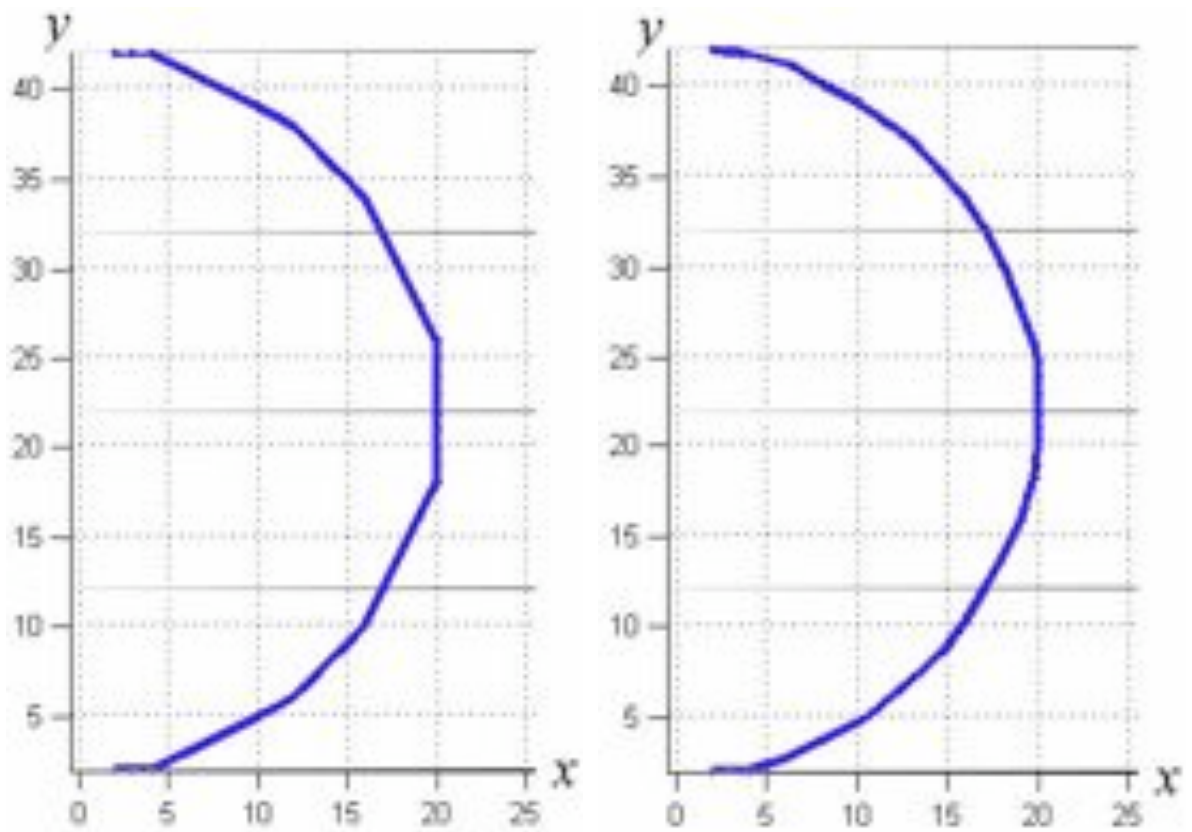


Fig. 11. The wave ray above the parabolic bottom slope, built using the proposed method. Initial approximation (left) and optimized by technique of variations (right).

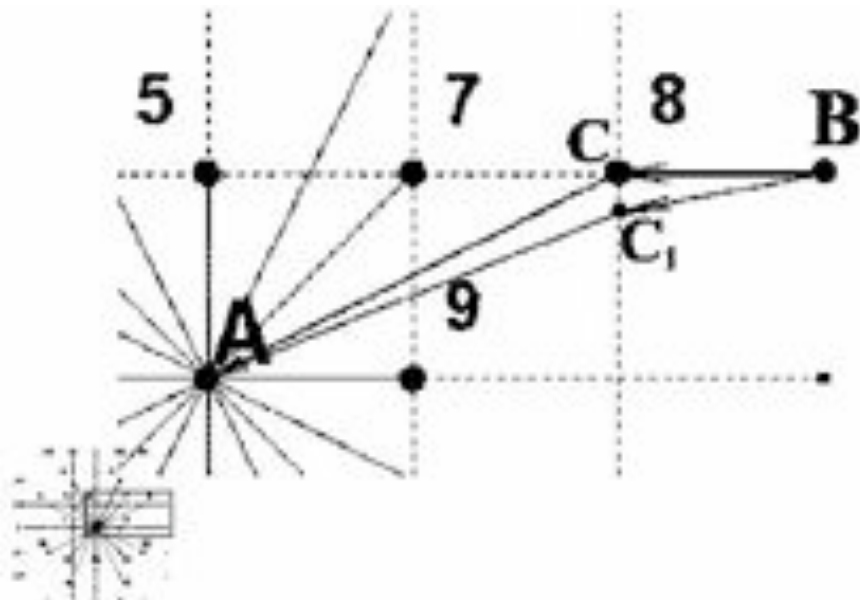


Fig. 12. The scheme of the travel-time correction algorithm.

The segment of a whole 16-dot template is shown in figure 12. The value of travel-time is to be determined at the grid-point **A**. The minimum travel time value at this point is obtained within a travel-time at the neighboring grid-point **C**. During previous computations the value of tsunami travel time at point **C** was determined using the time value at grid-point **B**. This can be taken from analysis of arrays $n_x(i, j)$ and $n_y(i, j)$. So, the value at point **A** was obtained as the sum of travel-time value at point **B**, plus the wave travel times along segments **BC** and **CA**. Then the possibility for the more optimal trajectory of the wave ray must be examined. By relocating point **C**, it is possible to find a new location of the intermediate point C_1 which can give the minimum travel time between point **B** and the grid-point **A**. Finally this travel-time (along the trace BC_1A) is to be accepted as the corrected travel time at the grid-point **A**. Using such an optimization procedure the test travel-time computations were carried out for an area of constant water depth. The small round tsunami source is situated in the center of the area defined by 1,000 by 1,000 grid-points. After determination of travel times at all grid-points, tsunami isochrones for every 250 sec of propagation were drawn. The shapes of isochrones by this method are much smoother than for the test without optimization (fig. 9). At some points of the computational area, the travel-time values differ by up to one minute for every one-hour of tsunami wave propagation time. So, for distant tsunamis this error can be significant, which means that the tsunami impact can occur at least a few minutes earlier than that predicted by traditional methods.

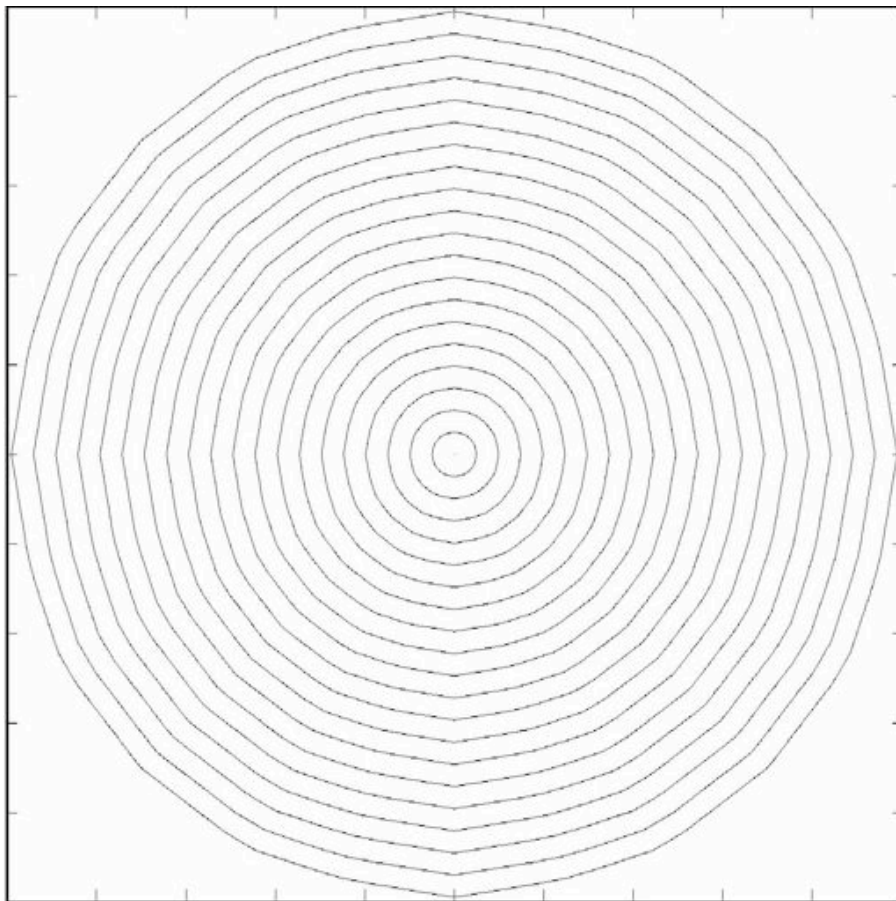


Fig. 13. Test isochrones computation in the area of constant depth using sixteen-dot template with the correction procedure (compare with the Figure 9).

CONCLUSION

A more effective method for solving the wave ray boundary value problem was proposed and tested. The method uses the results of numerical computation of wave travel-times from the source to all other grid points. The method was tested with known exact analytical solutions. Above a flat ocean bottom the time difference between the traditional 16-dot template method and the modified one is estimated to be up to one minute for every one hour of tsunami wave propagation. The proposed method is very effective for wave-ray calculation in 2-D and 3-D non-homogeneous media.

ACKNOWLEDGMENTS

The work was supported by SBRAS Grant for Integration project No. 2006/113, FASI-CRDF contract No. 02.434.11.7016 and RFBR grants 08-05-00300, 08-07-00105.

REFERENCES

1. Marchuk An.G., Chubarov L.B., Shokin Yu.I. Numerical modeling of tsunami waves. Siberian Branch of Nauka Publishers, Novosibirsk, 1983, 175 p. (In Russian).
2. Marchuk An.G. Rules of application of algorithms for tsunami waves kinematic computations that are based on Huygens' principle. Bulletin of the Novosibirsk Computing Center. Series: Mathematical Problems in Geophysics, Novosibirsk, ICM&MG SD RAS, Issue.5, 1999, p. 93-103.

ASSESSMENT OF THE IMPACT OF THE TSUNAMI OF DECEMBER 26, 2004 ON THE NEAR-SHORE BATHYMETRY OF THE KALPAKKAM COAST, EAST COAST OF INDIA

C. Anandan* and P. Sasidhar

Safety Research Institute,
Atomic Energy Regulatory Board, Govt. of India,
Kalpakkam
India

*e-mail: srianandan@igcar.gov.in

ABSTRACT

The devastating impact of the December 26, 2004 tsunami on the coast of South India has been well documented. However, only a few studies assessed the tsunami's impact in the near-shore region. The present study evaluates changes in bathymetry along the near-shore of Kalpakkam before and after the tsunami. Using GIS software, data was extracted from charts to create three-dimensional bathymetric representations of the offshore region before and after the tsunami. Initially, a TIN (Triangulated Irregular Network) surface was created by using Arc GIS software. Subsequently, by employing a 3D analyst tool, a three-dimensional surface of the near shore bathymetry was generated and comparisons were made with the pre-tsunami bathymetry. Based on comparisons of selected profiles, conclusions were drawn as to changes that resulted from the tsunami's impact. The analysis indicated that the tsunami deposited loose inner shelf sediments that altered significantly the near shore region bathymetry of the Kalpakkam coastal region. Sediment accretion changed the local bathymetry by 10 to 50 cm.

KEY WORDS: Bathymetry, Kalpakkam, GIS TIN, 3D surface, Tsunami impact

Science of Tsunami Hazards, Vol. 27, No. 4, page 26 (2008)

1.0 INTRODUCTION

The Tsunami of December 26, 2004 caused devastation to several countries bordering the Indian Ocean. The tsunami's various aspects and impact on coastal communities were extensively researched, surveyed, and documented (Tamil Nadu Govt. Tsunami Report, 2006; Rajamanikkam, 2006; Tamil Nadu Govt. Tsunami Report, 2006). Only a few of these studies assessed the impact on near-shore bathymetry.

Surveys carried out by several scientific groups in India documented that tsunami inundation varied from 200 to 600 meters inland along the coasts, but that at some locations the inundation was up to 2 km inland (Sasidhar, 2005, Rajamanikkam, 2006). The wide spatial variation in inundation and the observed run-up were attributed to variances in land topography and offshore bathymetry. A field survey by India's Geologic Survey (GSI, 2006) revealed that significant morphologic and structural changes of the seafloor were caused by the tsunamigenic earthquake along the Andaman-Nicobar ridge. Additional investigations at Port Blair and elsewhere in the Andaman and Nicobar islands (Rajamanikkam et al., 2006) determined that the sea level had been elevated by about one meter - which indicated subduction - whereas at other areas along the western coast of the middle Andaman Islands emergence of shallow coral beaches suggested uplift. Elsewhere, surveys of beach profiles at Puthu Vypeen, and Kerala (Rasheed et al., 2006) documented that the tsunami caused erosion of the foreshore and backshore coastal areas and landward transport of sediments.

In the South Andaman and Nicobar islands, studies (Subramanian *et al.*, 2006) concluded that land subsidence contributed to greater tsunami inundation. The survey indicated 0.8 m subsidence around Port Blair and 1.3 m subsidence in Great Nicobar. In contrast, a study of micro faunal distribution in sediments carried out along the Andhra Pradesh coast (Prasad et al., 2006) found no evidence of migration of deep-water fauna to the near shore regions. In general however, there was a change of depth contours towards the shore which indicated that the tsunami caused coastal erosion and deepening of the inner-shelf. A bathymetric survey along the Kerala coast (Prakash et al., 2006) indicated tsunami-induced erosion, even in the inner self of the Thangasseri, Vallikavu region and south of Kayamkulam of Kerala.

The near shore changes reported at several coastal areas (Seralathan et al. 2006; Hussain et al. 2006; Thakur and Kumar, 2007) prompted the initiation of this study for the Kalpakkam area - which houses several vital infrastructure installations. The main objective of the investigation was the generation of 3D seabed bathymetry in the near shore area before and after the tsunami for the purpose of identifying changes in the near shore bathymetry of Kalpakkam and the assessment of potential changes and impact from a future tsunami event.

2.0 STUDY AREA DETAILS

To accomplish the above-stated objectives, a coastal stretch of 4.5 km in length and 2 km in width was selected along the coast of Kalpakkam. The study area is bounded by the coordinates 80°10.'32E, 12° 34.'45 N to 80° 12.'33E, 12°32.'40N.

2.1 Coastal morphology

The coastline in this region is relatively flat and the foreshore is primarily composed of coarse sand. Isolated rocks can be found in the northern portion of the offshore area. A small stream named “Edaiyur” and a canal named “Buckingham” connect to the sea in the study area.

2.2 Seabed topography

The seabed within the survey area was generally less undulated with a gentle gradient sloping eastward and rock patches found in the northern portion. The seabed in other parts of the study area was generally smooth, dominated by micro-sand ripples aligned perpendicularly to the general direction of the littoral current and with a few patches of marine flora - which were identified. The samples collected from the seabed were composed of fine sand, shells, silt, mud and clay in varying proportions and particle sizes. The depth of the sea in the study area ranged from -0.17m to -14.40 m below the MSL datum.

3.0 MATERIALS AND METHODS

The National Hydrographic Officer (Dehradun) provided bathymetric data along the Kalpakkam coast for different dates before and after the 2004 tsunami struck the region. Specifically, the bathymetry data was extracted from charts of the decimeter scale that had been generated in January 2002 and anew in April 2005, after the tsunami. The bathymetric data sets were transformed to a common horizontal and vertical datum (Universal Transverse Mercator Projection, WGS-84 Datum) before being processed by GIS software. Subsequently, the data was recorded in the form of x, y and z parameters, corresponding to latitude, longitude and water depth. Using the ArcGIS software, digital databases were created for both the pre and post-tsunami bathymetry for the selected 4.5 km block segment of the coastline, extending 2 km out to sea. In general, two common surfaces i.e. the Triangulated Irregular Network (TIN) and GRID were used to represent the bathymetry surface. Since TIN is the recommended method to use in creating accurate model surfaces from hydrographic data (Byrnes et al. 2002), TIN and the 3D analyst extension of Arc Info software were used to generate both pre and post tsunami 3D surfaces from the digital data and thus determine changes in submarine topography caused by the tsunami.

4.0 RESULTS AND DISCUSSION

The 3D surface of the near shore seabed of the Kalpakkam coastline indicates that the area is generally less undulated, with a gentle gradient sloping towards the east. Also, in the northern part small projections were noticed and identified as rock patches. There are no artificial features and no wrecks of any kind exist in this area (Fig. 1). The elevation of the sea surface ranges from -0.4m to -13.0 m below MSL (Fig. 1a) in the pre- tsunami period and from -0.1 m to -14.0 m below MSL (Fig. 1b) in the post- tsunami period, respectively.

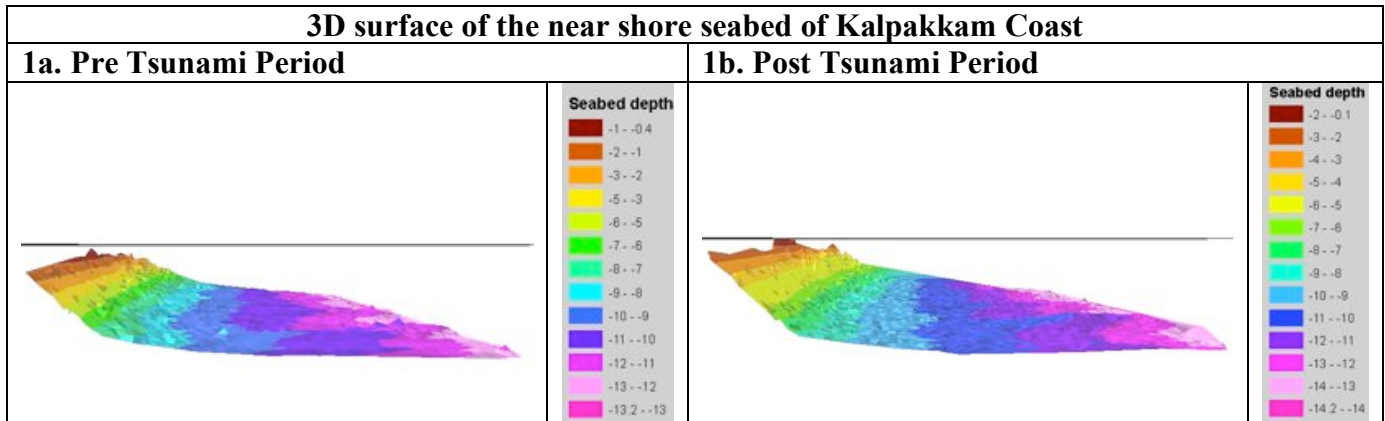


Fig. 1 Pre- and Post- tsunami Seabed surface of the Kalpakkam Sea

4.1 Changes in near shore Bathymetry due to Tsunami

By comparing pre and post tsunami seabed surfaces, it was determined that the seabed became shallow near the coast at most locations, suggesting deposition of inner shelf or deep-sea sediments in the shallow areas. Siltation at a typical transect was measured to be in the range of 10 cm to 50 cm (from 9 out of 15 locations) (Table-1). Sporadic traces of Monazite deposits were also found in this area up to 100 m off the shoreline. The deposition of beach sands in some dwelling units up to 500 m inland, demonstrates also the deposition of inner shelf sediments in the area (Seralathan et al. 2006; Hussain et al. 2006; Anandan et al., 2006) by the tsunami. Also at some areas (in 6 out of 15 locations), the seabed eroded, as it can be seen from Table-1 data. Similar accretion rates ranging from 10 to 60 centimeters were also noticed at various inlets of the Kayankulam and Kollam region and were attributed to the tsunami (Prakash et al., 2006). Average accretion rates of 2 cm/year have been reported for areas near islands of the Gulf of Mannar for the pre-tsunami period (Thanikachalam & Ramachandran, 2003). Considering a similar accretion rate of 2 cm/year due to siltation, the study area at the Kalpakkam coast would have resulted in 6 cm of change between 2002-2005, whereas the study shows that a change of 10 to 50 cm had occurred, which implies that this could be due to the tsunami impact, which included the expected normal siltation. Furthermore, the siltation levels recorded at Kalpakkam were in agreement with those determined for the Kayankulam and Kollam areas (Prakash et al., 2006).

Table 1 Pre and Post bathymetry along a typical profile (Measurement along Profile-IV up to 500m)

Sl.No.	Depth measurement at a typical profile	Pre bathymetry (m)	Post bathymetry (m)	Difference in bathymetry (m)*
	a	b	c	d= b-c
1.	Point1	2.2	1.7	-0.50
2.	Point2	3.8	3.9	+0.10
3.	Point3	4.3	3.8	-0.50
4.	Point4	4.6	4.1	-0.50
5.	Point5	6.3	5.8	-0.50
6.	Point6	6.9	6.6	-0.30
7.	Point7	6.6	6.7	+0.10
8.	Point8	6.7	7.2	+0.50
9.	Point9	6.8	7.0	+0.20
10.	Point10	7.0	7.4	+0.40
11.	Point11	7.1	7.0	-0.10
12.	Point12	7.3	7.0	-0.30
13.	Point13	7.5	7.8	+0.30
14.	Point14	7.8	7.3	-0.50
15.	Point15	8.0	7.8	-0.20

* (-) decrease in depth (deposition): (+) increase in depth (erosion)

4.2 Profiles

To visualize the changes in seabed due to the 2004 tsunami, four profiles (Profile I – IV) were chosen for both the pre- and post- tsunami seabed. These four profiles are shown in Figure 2. At a distance of 125 m from the coastline the slope of the seabed were measured for the pre and post tsunami period for all four profiles.

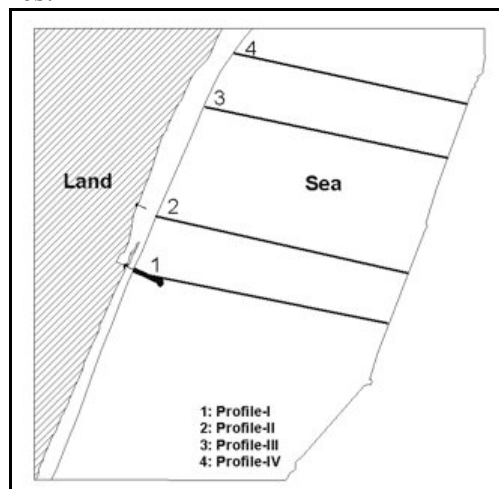
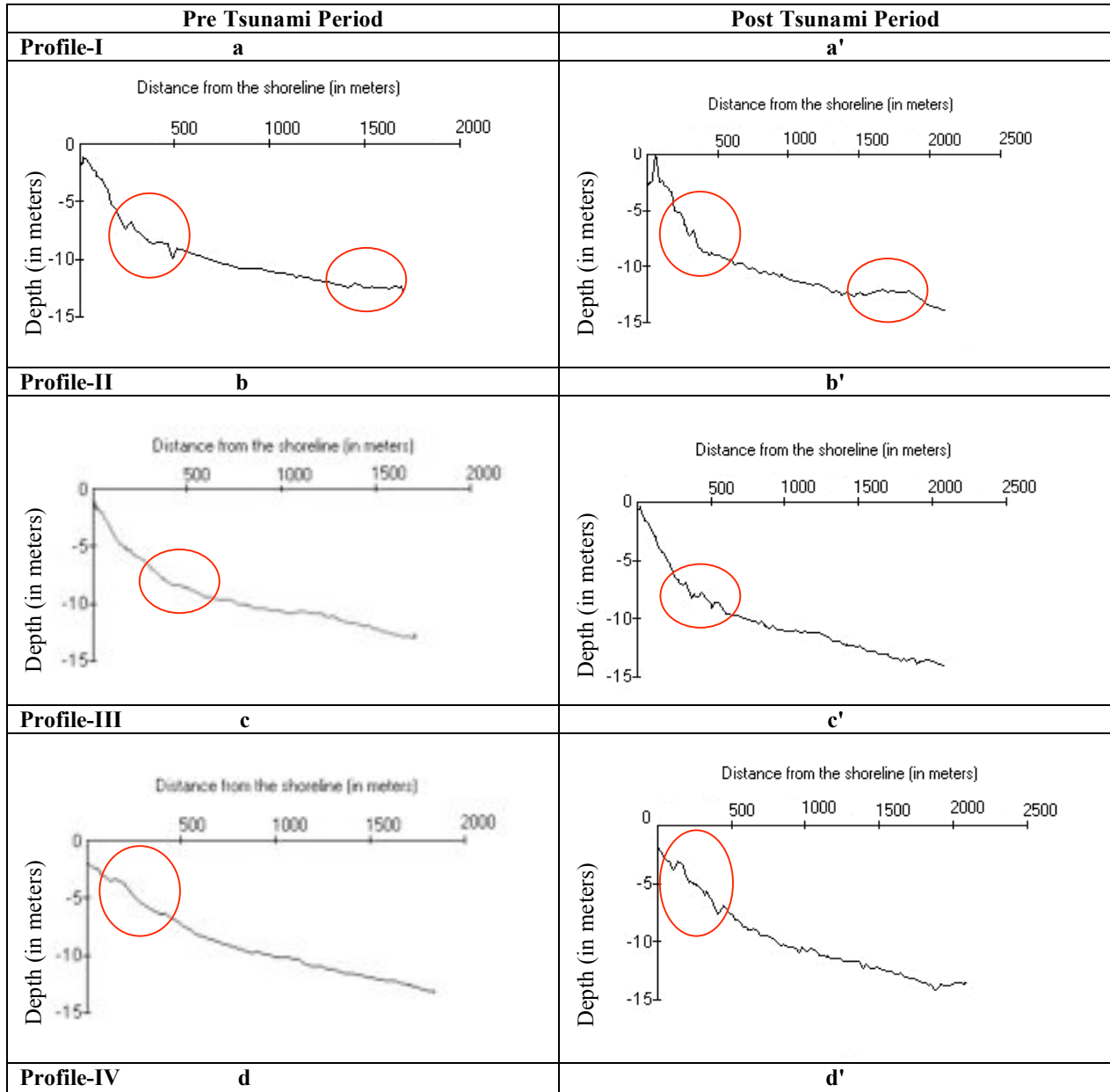


Fig. 2 Locations of the profiles I to IV

4.2.1 Profile - I:

A depression was found at a distance of 500m from the shoreline along Profile-I for the pre tsunami period. After the tsunami this depression was found to be filled up which that supports the tsunami's depositional phase. Deposition was also observed in the post tsunami seabed along the same transect at a distance of 1500 to 2000 meters from shoreline, which also supports the depositional phase of the tsunami. The increase in the slope of seabed for the post tsunami profile as compared to the pre tsunami baseline condition, corroborates the earlier findings. (Fig. 3a & Fig. 3a', Table -2)



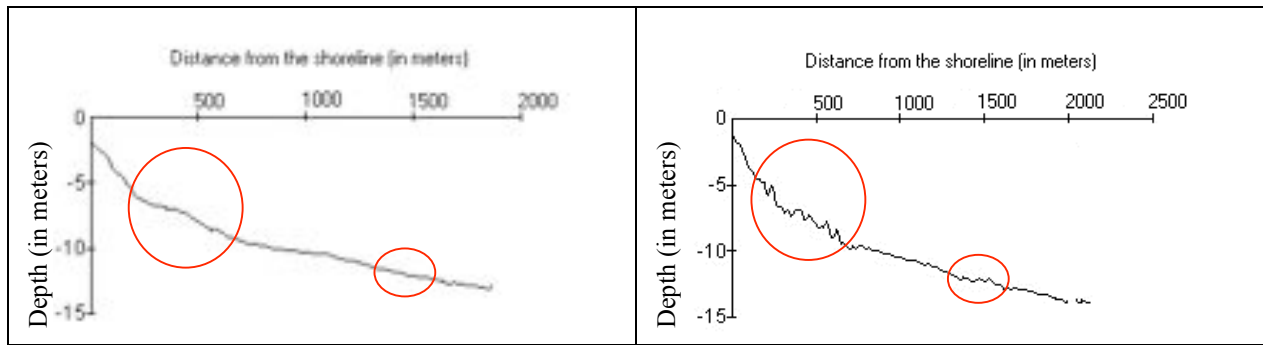


Fig. 3 Profiles shows the areas of changes in the bathymetry (highlighted in the circles)

Table 2. Seabed slope in pre and post tsunami phases along four profiles

Sl.No.	Location	Pre-tsunami Slope angle*	Post-tsunami Slope angle*	Difference in the slope angle
1	Profile-I	60°	65°	+5°
2	Profile-II	58°	63°	+5°
3	Profile-III	34°	44°	+10°
4	Profile-IV	48°	58°	+10°

*Seabed angle measured at a distance of 125 m from the shore line in all profiles

3.2.2 Profile – II:

Profile-II shows that along this transect at a distance of 400m to 600m from the shoreline the seabed was undulated in the post tsunami bathymetry as compared to the pre-tsunami bathymetry - which implies seabed erosion by the tsunami. Also, the slope of the seabed was steeper compared to the pre tsunami profile, which support huge deposition of sediments (Fig. 3b & Fig. 3b', Table-2).

4.2.5 Profile – III:

Profile-III shows that the seabed was undulated at a distance ranging between 100 to 400 meters from the shoreline and that at a distance of 1000 meters from the shoreline the seabed was again undulated in the post tsunami bathymetry - when compared to the pre tsunami bathymetry. Further along the profile of this transect the seabed was undulated in the post-tsunami bathymetry compared to the pre-tsunami bathymetry, which again implies the erosional phase of the tsunami in this area. The steepness of the slope for the post-tsunami profile implies deposition of inner shore sediments along the coast. (Fig. 3c & Fig. 3c', Table-2)

4.2.6 Profile – IV:

Profile-IV shows the sea bed to be highly undulated at a distance of 250 to 750 meters from the shoreline in the post tsunami period. Similarly, at a distance of 1500 meters the seabed was again undulated. The steepness of the slope as compared to the pre-tsunami slope, implies bulk deposition of inner shore sediments (Fig. 3d & Fig. 3d', Table-2).

In summary, the shallowness in the seabed due to the deposition of deep sea or inner shore sediments in all of the profiles indicates the depositional phase of the tsunami waves, whereas, in only a few locations the seabed was deepened (Table-1). The present study supports that local bathymetry as well as coastal morphology of an area play major roles in controlling the tsunami wave impact. This was also supported by studies of many other coastal areas of India (Rasheed et al. 2006; Prakash et al., 2006).

5.0 CONCLUSIONS

The above study assesses the impact of the 2004 tsunami on the near-shore seabed of Kalpakkam by employing the pre- and post- tsunami bathymetry data. The study supports that sediment accretion in the range of 10 cm to 50 cm occurred in the nearshore area of the Kalpakkam Sea. The field observations support the deposition of loose inner shelf sediments by the tsunami and emphasize the importance of periodic baseline surveys of near shore bathymetry to determine changes. Comparison of baseline digital bathymetric data for the same area can provide an effective method for calculating the net movement of sediments, either by accretion or erosion, and help quantify temporal changes in bathymetry by such processes, as well as determine sediment transport pathways and volumetric estimates of sediment budgets, in general. Such evaluation of changes in the near shore bathymetry are important in view of the amounts of water that is needed by the underwater intakes of the condenser cooling system of the Madras Atomic Power Station (MAPS) in the coastal area of Kalpakkam. Assuring seawater availability is necessary for the condenser coolant refinement, at least for three decades, for the safe operation of the nuclear power plant. This need for safe operations of nuclear power stations warrants close scrutiny of bathymetry changes of the offshore areas where such plants are located. Also, the present study indicates the importance of GIS software in assessing the impact of natural disasters through 3D plots in real world coordinates, and specifically in this case, in evaluating bathymetry changes due to a tsunami.

ACKNOWLEDGEMENTS

The authors express their sincere thanks to the Civil Engineering Division, IGCAR, Government of India for their co-operation in generation of the refined database and to Dr. George Pararas-Carayannis, for help in clarifying further the above described study.

REFERENCES

- Abdul Rasheed, K. A., Kesava Das, V., Ravichandran, C., Vijayan, P.R. and Tony, J. Thottam. (2006). Tsunami Impacts on Morphology of Beaches along South Kerala Coast, West Coast of India. *Science of Tsunami Hazards*, Vol. 24, No. 1, page 25-34.
- Anandan, C., Sasidhar, P., Akila, S. and Kannan, S.E. (2006a). Role of Geoinformatics in assessing the impact of Tsunami at Kalpakkam Coast. In: Proceedings of the workshop on “Role of Armed Forces in Disaster Management” organized by College of Military Engineering, Pune during June 20-21, 2006.
- Byrnes, M.R., Baker, J.L. and Li, Feng (2002). Quantifying potential measurement errors associated with bathymetric change analysis. ERDC/CHL CETN-IV-50, U.S. Army Engineer Research and Development Center, Vicksburg, MS. (<http://chl.wes.army/library/publications/chetn>).
- GSI. (2006). Geological Survey of India. Post-Tsunami studies carried by Marine Wing of Geological Survey of India. 26th December 2004 Tsunami: Causes, Effects, Remedial measures, Pre and Post tsunami Disaster Management- A Geoscientific perspective. (ed.G.V.Rajamanickam). New Academic Publishers, New Delhi. Pp.177-182.
- Hussain, S.M., Suresh Gandhi, M. Krishnamurthy, R.K. and Bagendra, R. (2006). Micropaleontological Investigations of Tsunami sediments of Tamil Nadu and Andaman Islands. 26th December 2004 Tsunami: Causes, Effects, Remedial measures, Pre and Post tsunami Disaster Management- A Geoscientific perspective. (ed.G.V.Rajamanickam). New Academic Publishers, New Delhi. Pp. 83-115.
- Matsuyama, Masafumi, Walsh, J.P. and Yeh Harry. (1999). The effect of bathymetry on tsunami characteristics at Sisano Lagoon, Papua New Guinea. *Geophysical Research Letters*, Volume 26, Issue 23, p. 3513-3516.
- Prakash, T.N., Chattopadhyay, S. and Nair, A.S.K. (2006). Impact of Tsunami on the Kerala Coast and Rehabilitation Plan for the worst affected stretch at Alappad. 26th December 2004 Tsunami: Causes, Effects, Remedial measures, Pre and Post tsunami Disaster Management- A Geoscientific perspective. (ed.G.V.Rajamanickam). New Academic Publishers, New Delhi. Pp.150-174.
- Rajendra Prasad, P. et al. (2006). Effect of 26th December 2004 Tsunami along the Andhra Coast – an Integrated Study. 26th December 2004 Tsunami: Causes, Effects, Remedial measures, Pre and Post tsunami Disaster Management- A Geoscientific perspective. (ed.G.V.Rajamanickam). New Academic Publishers, New Delhi. Pp.116-138.
- Sasidhar, P. and Anandan, C. (2005) Inundation Zone Mapping at Kalpakkam using RS and GIS techniques, Internal Report, SRI/AERB/August 05, 2005/IR1.

- Seralathan, P. et al. (2006). Post Tsunami sediment characterization of Tamil Nadu coast. 26th December 2004 Tsunami: Causes, Effects, Remedial measures, Pre and Post tsunami Disaster Management- A Geoscientific perspective. (ed.G.V.Rajamanickam). New Academic Publishers, New Delhi. Pp. 59-82.
- Subramanian, B.R. et al. (2006). Inundation of Seawater due to the Indian Ocean Tsunami along the Indian Coast. 26th December 2004 Tsunami: Causes, Effects, Remedial measures, Pre and Post tsunami Disaster Management- A Geoscientific perspective. (ed.G.V.Rajamanickam). New Academic Publishers, New Delhi. Pp.10-44.
- Victor Rajamanickam, G. and Prithviraj, M. (2006). Great Indian Tsunami: Indian Prospective. 26th December 2004 Tsunami: Causes, Effects, Remedial measures, Pre and Post tsunami Disaster Management- A Geoscientific perspective. (ed.G.V.Rajamanickam). New Academic Publishers, New Delhi. pp. 1-6.
- Tamil Nadu Govt. Tsunami Report, 2006. www.tn.gov.in/tsunami/. Official website of Government of Tamil Nadu.
- Thakur, N.K. and Pradeep Kumar, A. (2007). Role of bathymetry in tsunami devastation along the East Coast of India. *Current Science*, vol. 92, No. 4, 25 February 2007. 432-434 p.
- Thanikachalam, M., and Ramachandran, S. (2003). Monitoring Changes in Seafloor Morphology Using Multi-date Bathymetry data: A Case Study of the Gulf of Mannar, Southeast Coast of India. *Map Asia Conference*, 2003.
(<http://www.gisdevelopment.net/application/nrm/ocean/pdf/ma03009.pdf>).

TSUNAMI MITIGATION IN HAWAII

George D. Curtis

University of Hawai`i, Department of Ocean and Resource Engineering, 2450 Dole St.,
Honolulu HI, 96822
gcurtis@hawaii.edu

(For the conference on “Solutions to Coastal Disasters”, April 13, 2008; sponsored by ASCE)

ABSTRACT

Hawai`i has a long, though sporadic history of deadly tsunami attacks. Since the 1946 tsunami disaster the State of Hawaii has developed increasingly sophisticated and effective mitigation strategies. The evolution and operation of these strategies is described in this paper. Tsunamis will no longer be Hawai`i's deadliest natural hazard.

INTRODUCTION

The tragic 1946 tsunami, striking Hawai'i from the Aleutians, and killing 159 people, illustrated the problem of the tsunami-susceptible coastline. There was no warning system at that time. Tsunamis are the most deadly natural hazard affecting Hawai'i and good mitigation is critical. This paper discusses the development of mitigation efforts in Hawai'i and the implementation of the present system.

THE PROBLEM

Table 1. Relative hazards, last century (lives lost)

(Sources: Cox, Furumoto, Schmidt, Curtis)

<u>HAZARD</u> (last century)	<u>LIVES, TOTAL</u>	<u>LIVES, PER YEAR</u>
Earthquake	0	0
Volcano	1	.01
Hurricanes	<8	<1
Tsunami	234	2.5
Opihi gathering	?? Many	??
Auto	~4000+	~60+

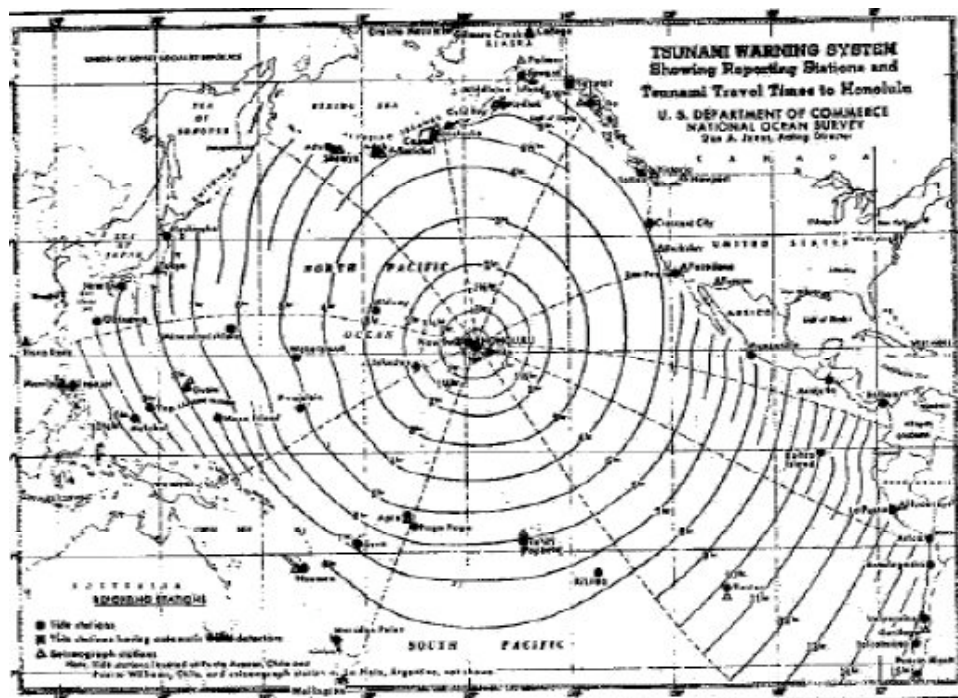


Fig. 1 Tsunami Travel Time Chart to Hawai'i

Although attempts to provide a tsunami warning based on seismographic data of the Hawaiian Volcano Observatory had been made (one was partly successful), the instruments were too slow and, furthermore, most of the large earthquakes do not necessarily generate tsunamis. Without timely confirmation of hazardous wave action, reliable tsunami warning was not feasible. Thus, coastal residents were vulnerable to this hazard.

Figure 1 illustrates how tsunamis approach Hawai'i from many directions, as well as the time available to evaluate the event, warn, and evacuate those in inundation zones.

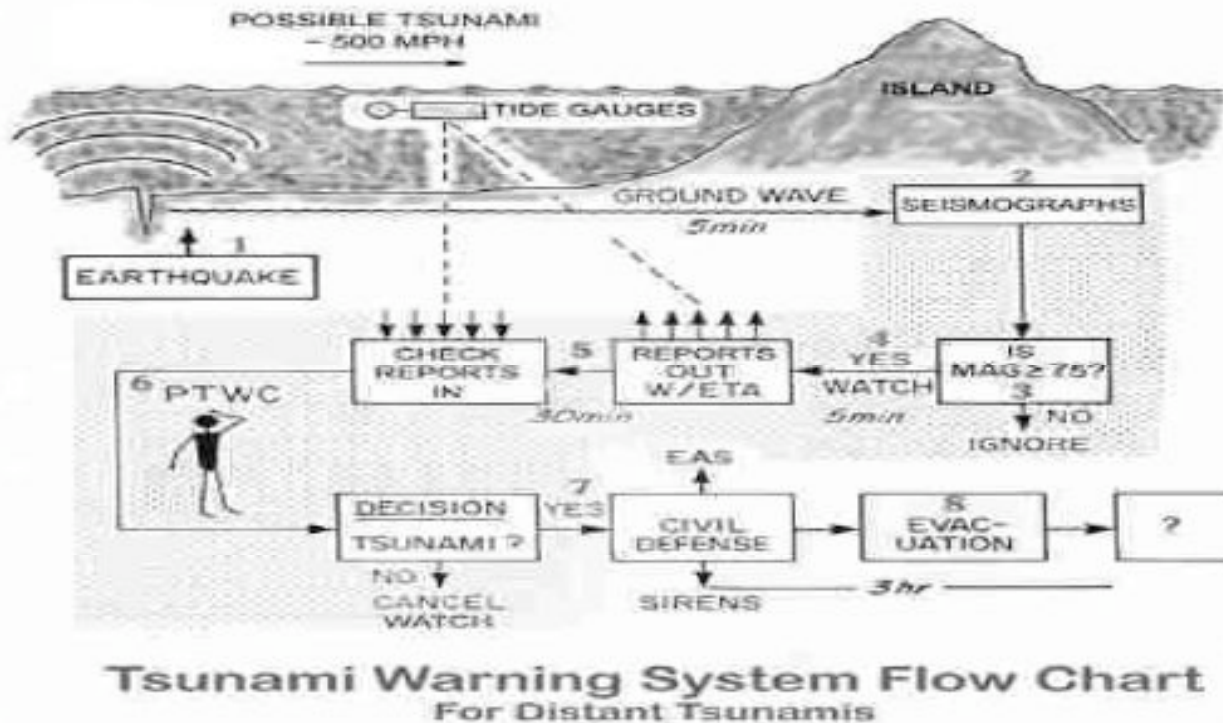


Fig. 2 Data and Action Flow in Tsunami Warning System

THE SOLUTIONS

Scientists began to take advantage of the World War II improvements in communications and instrumentation to help provide warning of distant tsunamis. By 1948, a basic tsunami warning system was in place at the U.S.G.S. Honolulu Observatory, using seismic information and verbal contact with tide gauge stations around the Pacific (Zetler, 1988). Over the years this capability has expanded to use more communications channels, observers, and seismic stations. Eventually this system became the Pacific Tsunami Warning Center (PTWC), which now encompasses 24 nation states.

In Hawai'i the State Civil Defense agency receives the watch and warning information from PTWC and coordinates the overall response; all islands proceed with warning simultaneously. The

preparation and evacuation is carried out by the four County Civil Defense agencies using police, fire, public works, Red Cross, national and state parks, and other available personnel. The watch period (during which a tsunami might be en route) begins six hours before expected arrival of the first wave. If the tsunami is forecast to be hazardous, the actual warning and evacuation starts three hours before first wave arrival.

Warnings were successful for the 1952 and 1957 tsunamis with no lives lost, but the strong attack of the 1960 tsunami from Chile showed the inadequacy of the evacuation and response to the warning. The 1960 tsunami caused more than 60 deaths in Hilo, for example. The rather high “false alarm” rate from the warning system contributed to the response problem with the public. Actually, there have been no false alarms; those were non-hazardous tsunamis, but this was seldom the public perception.

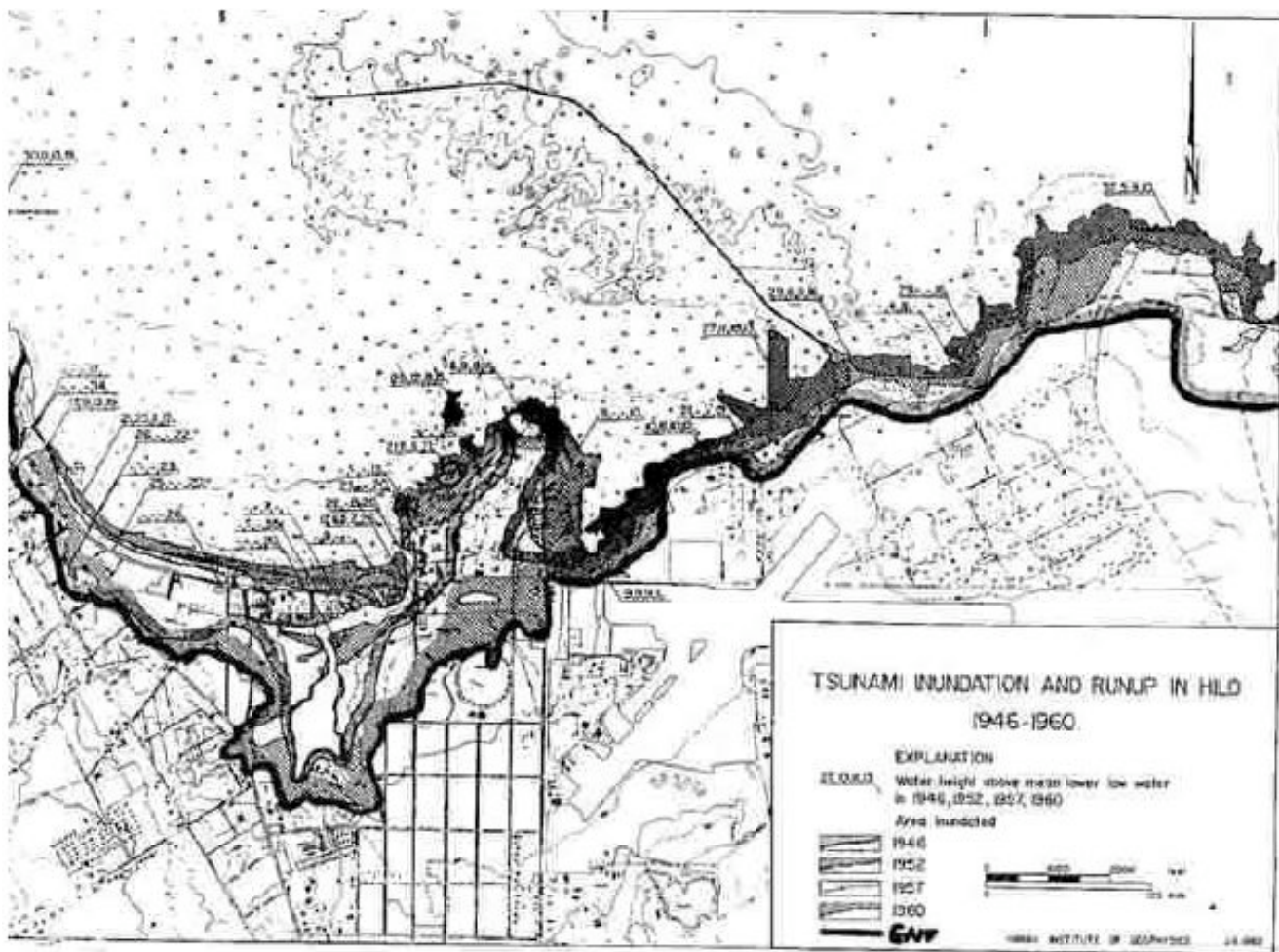


Fig. 3 Flooding in Hilo from Four Tsunamis

Because of the long, though sporadic history of tsunamis affecting the Hawaiian islands, both authorities and the public began additional steps to avoid further deaths and minimize damage to facilities. Using the historical run-up and wave action records gathered by tsunami researchers at the University of Hawai'i (UH) and published by Loomis (1976), Cox (1961) developed the initial, broad brush tsunami inundation maps for the Hawaiian islands. By 1963, these maps were published by Civil Defense and used for evacuation after they were placed in the phone books of each island. More coastal sirens were installed and both the State and County civil defense agencies made plans for better evacuation in the affected areas.

During this period, Vitousek (1961) proposed a deep sea tsunami wave detection system based on a sensor at the end of an unused undersea cable. Using a modified commercial pressure sensor, he successfully deployed the device on a cable offshore the island of Hawai'i. However, no funding was available at the time to deploy the actual deep ocean system. The Deep Ocean Assessment and Reporting of Tsunamis (DART) system has since successfully filled this need with deployment of a number of buoys in both the north and south Pacific.

An evacuation for the non-hazardous tsunami of 1986 showed major problems on O'ahu and the need for more improvements. An evacuation rehearsal is not feasible as it could be a hazard itself and costs presently more than \$50 million overall for the Hawaiian islands. The fortuitous warning served a valuable purpose, no one was injured during the evacuation – and it cost \$30 million.

Thereafter, updated, more detailed maps with smaller, more usable zones were developed using all historical runup and inundation records (Houston, 1977; Loomis, 1976) applied in a 1-D model developed earlier at the UH (Curtis, 1991). In addition, evacuation procedures were overhauled and the combination was found to work much better in the next evacuation, which occurred in 1994. (Fig. 4)

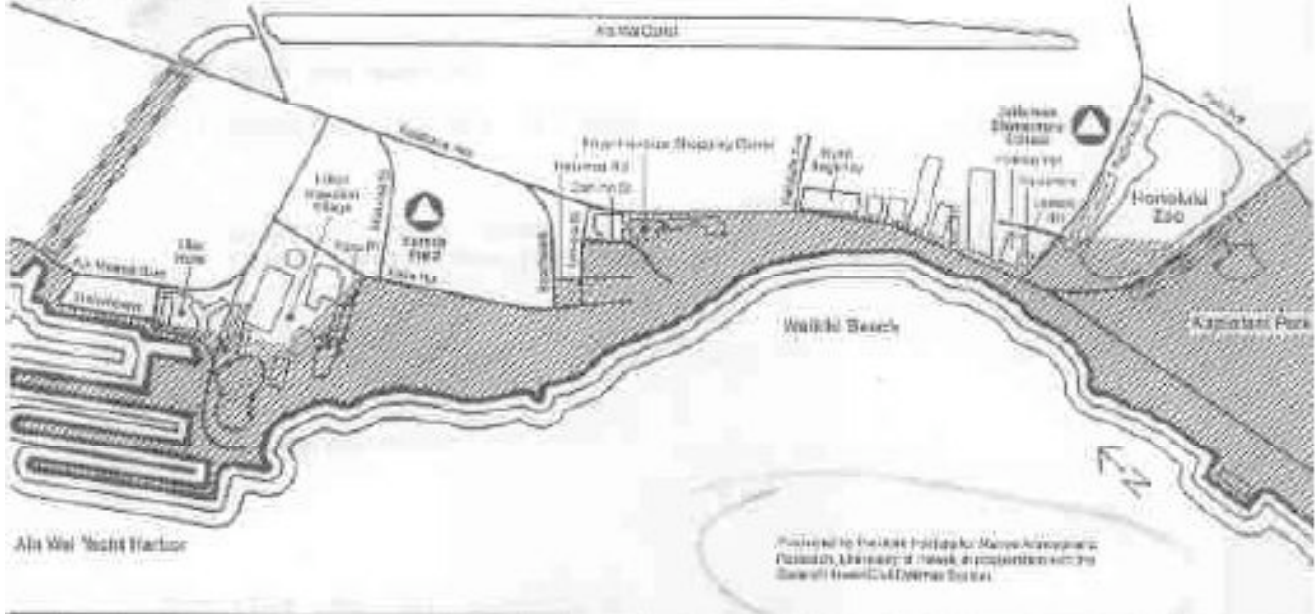
These precepts, the historical records, and the tsunami data developed under these programs are used presently for evaluation and validation of new and better numerical models (Wei, et al, 2006). They are being applied by the Ocean and Resource Engineering to upgrading Hawai'i inundation zones and to contribute to warning (Yamazaki, et al, 2006) and modeling methodology in other coastal areas under sponsorship of NOAA.

CONCLUSION

The tsunami warning system, which became the Pacific tsunami warning system, has never missed an event and has benefitted from numerous improvements, which have greatly reduced the perceived false alarm rate as well as providing faster analyses of the threat. A greatly improved urgent local warning system, involving real-time wave sensors in addition to seismic data, has been put in place. The rare tsunami originating in Hawai'i, allows very little time for evacuation.

Further improvements now under way include application of real-time models to DART and other data, (Curtis and Mader, 1987) refined and updated zones being developed with 2-D models, more public education, and trained observers available to provide vital data from the next event (Curtis, 1990). Generally good response procedures are in place. With these improvements, tsunami deaths can be kept to an absolute minimum.

Map 1: Waikiki



Map 2: Waikiki to Wailupe

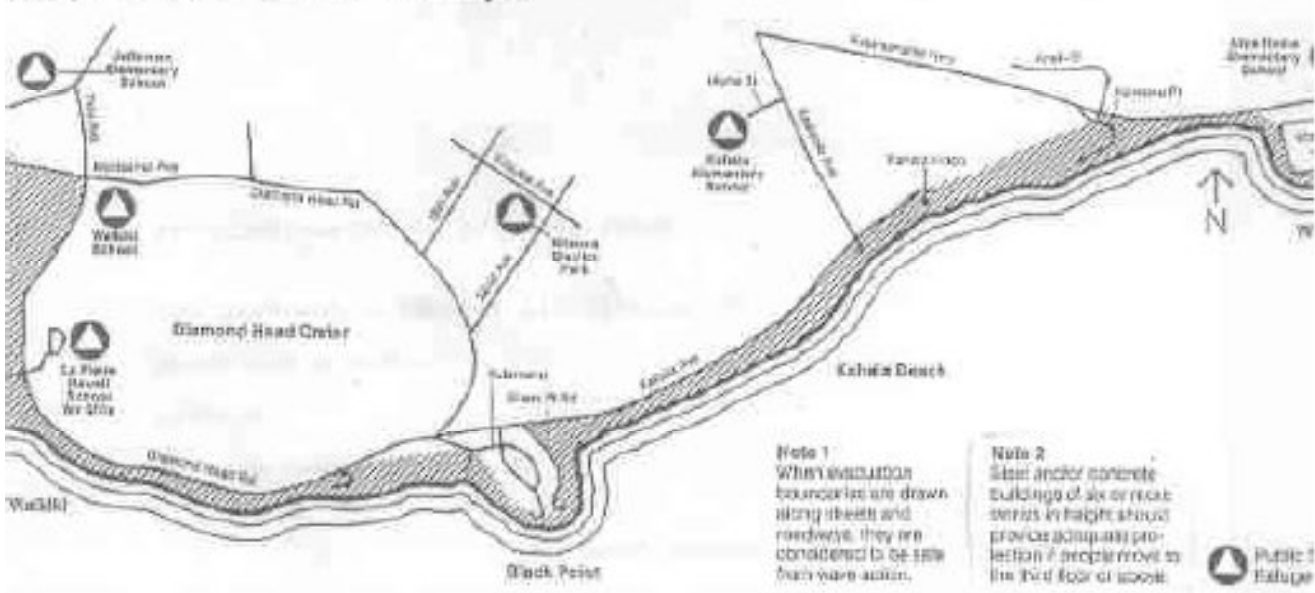


Fig. 4 Evacuation Maps from phone book

REFERENCES

- Cox, Doak C., Potential Tsunami Inundation Areas in Hawai`i, Univ. of Hawai`i, Hawai`i Institute of Geophysics, Honolulu, HI, Rept. No. HIG-14, 1961, 26 pp.
- Cox, Doak C., Tsunami Height-Frequency Relationship at Hilo, Hawai`i, Hawai`i Inst. Geophysics, Univ. Hawai`i, Honolulu, Informal report, 1964.
- Curtis, George, and Charles Mader, "Real-time Monitoring and Modeling for Tsunami Threat Evaluation", *Science of Tsunami Hazards*, Vol. 5, No. 1, 1987, pp. 49-55.
- Curtis, George, "A Methodology for Developing Tsunami Inundation and Evacuation Zones", Proc. of the Pacific Congress on Marine Technology, Tokyo, July 1990.
- Houston, J.R., R.D. Carver, and D.G. Markle, Tsunami-Wave Elevation Frequency of Occurrence on the Hawaiian Islands, U.S. Army Corps of Engineers, Waterways Experiment Station, Vicksburg, MS, Tech. Rept. H-77-16, Aug. 1977, 63 pp. and 42 plates
- Loomis, H.G., Tsunami Wave Runup Heights in Hawai`i, Univ. of Hawai`i, Hawai`i Institute of Geophysics, Honolulu, HI, Rept. No. HIG-76-5, May 1976, 95 pp.
- Vitousek, M.J., "Proposed Mid-ocean Tsunami Gage and Oceanography Instrument System". Proc. Tsunami Meetings Associated with Tenth Pacific Science Congress, Honolulu, HI, 1961, ed. Doak C. Cox, IUGG Monograph No. 24, July 1963, Paris, pp. 131-133.
- Wei, Y.; Mao, X.Z.; and Cheung, K.F. (2006), "Well-balanced finite Volume Model for Long Wave Runup", *Jour. Waterway, Port, Coastal, and Ocean Engineering*, 132(2),114-124.
- Yamazaki, Yoshuki, Yong Wei, Kwok Fai Ceung, and George Curtis, "Forecast of Tsunamis from the Japan-Kuril-Kamchatka Source Region, *Natural Hazards*, Vol. 38, No. 3, July 2006
- Zetler, B.D., "Some Tsunami Memories", *Science of Tsunami Hazards*, Vol. 6, 1988, pp. 57-71.

**OBSERVED INFERENCES FROM SUDDEN CHANGES IN THE
SEDIMENTOLOGICAL PROCESSES DURING THE DECEMBER 26, 2004 TSUNAMI
ALONG THE EAST COAST OF INDIA**

Loveson, V. J.

Central Institute of Mining & Fuel Research, Dhanbad – 826 001.

Angusamy, N.

Tamil University, Thanjavur – 613 005.

Gujar, A. R.

Geological Oceanography Division, National Institute of Oceanography, Dona Paula,
Goa – 403 004

Chandrasekar, N.

Centre for Geotechnology, Manonmaniam Sundaranar University,
Abishekhapatti, Tirunelveli - 627 012

Rajamanickam, G. V.

Department of Disaster Management, SASTRA University, Thanjavur – 613 402.

ABSTRACT

In connection with observations made on the impact of beach placer mining, a study area extending from Poompuhar to Nagoor, in Tamil Nadu, had been chosen for regular profiling and sediment sampling since April 2003. The on-set of the tsunami of 26th December 2004 encouraged continuation of the study in order to understand the sudden changes in the sedimentological processes caused by this tsunami. As a profiling survey of the area had been completed on 16th December 2004, an exact quantum of erosion level caused by the tsunami was determined for several stations. Except for Nagoor, all other stations showed erosion of the beaches, with a maximum of 2.5 m, particularly in the Karaikkal area. The study identified two major geomorphologic parts, the first extending from northern Poompuhar to Karaikkal and the second from southern Karaikkal to Nagoor. Changes in the geomorphologic characters observed at these two areas were attributed to the nature of the inner shelf bathymetry. The different beach profiles for the pre- and post-tsunami periods that were prepared through trend analysis, clearly show huge deposition of sediments on the Nagoor beaches. The influence of inlets in Karaikkal, Poompuhar and Nagoor are strongly indicated by the nature of sediments that were deposited on beaches at these locations. When the sediment texture of pre-tsunami deposits is compared with that of post-tsunami deposits, a characteristic shift in kurtosis is observed on all the beaches, while skewness and mean establish a shift on beaches that eroded. Examination of heavy mineral composition in sediments indicates a dramatic shift in concentration, ranging from 19 to 76 % in the Nagoor area. Further study of sedimentological process may shed additional light on tsunami impacts on any beach in the study area, particularly because of the ongoing monitoring and the availability of past baseline records.

Keywords: Tsunami, Coastal areas, Sediments, Mineral compositions

Science of Tsunami Hazards, Vol. 27, No. 4, page 43 (2008)

1. Introduction

Worldwide tsunami impacts of the last century have been documented by many researchers (Heck, 1947; Iida et al., 1967; Nakata et al, 1993; Lander and Whiteside, 1997; NGDC, 2001 and Shi et al 1995, Maramai et.al., 2005; McMurtry et. al., 2004; Scheffers and Kelletat, 2003; Tappin et.al., 2001; Nanayama et. al., 2000; Clague et.al., 2000; Dominey-Howes et. al., 2000; Papadopoulos and Chalkis 1984; Monge and Mendoza, 1993; Mörner, 1999). In most cases, post tsunami collected data was used for evaluation and assessment. The present study discusses the erosional and depositional processes in a coastal area of India, before and after the tsunami of 26th December 2004. The tsunami brought sudden changes in sedimentological processes and resulted in transformations of coastal landforms, which also affected the quality of life. The huge amount of erosion that occurred in the foreshore and backshore areas, created drastic changes of the coastal geomorphology, thus necessitating also a new approach to coastal management for this area.

Since April 2003, there was an ongoing project in the study area relating to the impact of placer mining so, profiles were monitored regularly and samples were collected fortnightly. A complete set of geological observations, such as beach profiling, wave numbers, wave failures, littoral drift, sediment texture, heavy mineral distribution, etc., in the tsunami worst affected area, i.e., were collected fortnightly for more than a year, up to December 2004. Such detailed baseline data enabled the assessment of post tsunami changes on sediments and sedimentation processes in this coastal zone. In the recent years, in spite of frequent cyclones, there had been no drastic changes or massive transportation of beach sediments either inland or offshore, except for those caused by the 1999 super-cyclone Orissa in the northern part of the east coast of India. However, the 2004 tsunami caused large and abnormal changes along the Nagapattinam coast. The present paper discusses the nature of changes in sediment composition and transport and in coastal landforms that were caused by the tsunami.

2. The Study area

A survey of the coastal sector between Poempuhar and Nagoor of Nagapattinam district, Tamil Nadu (Figure 1) had been carried since December 2003 for the purpose of understanding the potential environmental impact of proposed beach placer mining. Within this 35 km coastal distance, 8 profiling stations were maintained at intervals of 5 km. A permanent benchmark was fixed at each profiling station and beach profiling was conducted fortnightly since December 2003. The last profiling was completed on 16th December 2004 before the tsunami struck. Similarly, sand sampling was also done at each station at intervals of 5 m along each profiling track. Briefly after the tsunami, on 7th January 2005, another profiling was done after re-checking and re-fixing the benchmark. There were drastic shifts in erosional levels at all stations except for Nagoor. Out of the five stations where measurements were made, at Karaikkal there was 2.5 m change in erosion level, whereas at Poempuhar and Kottucherimedu the erosion levels were 0.5 m to 1.5 m respectively at high tide, and at Chinnankudi and Chandirapadi there was only a marginal change.

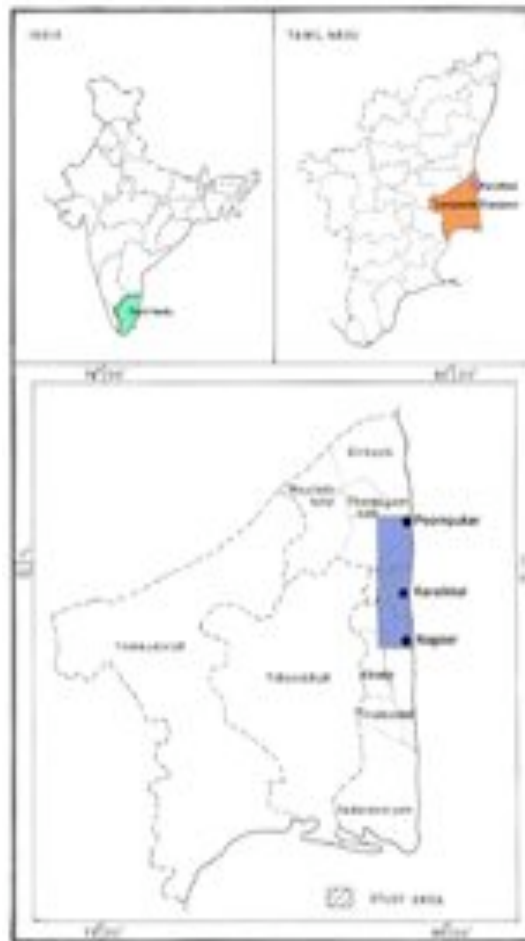


Figure 1. Study Area

3. Coastal Geomorphology and Shelf Characteristics

The study area has a straight coastline trending in N-S direction. After the tsunami, the geomorphologic characters the area was divided into two significant geomorphologic parts viz., Poompuhar to Karaikkal (PK) and Karaikkal to Nagoor (KN). The PK area has wider coastal extent with four massive beach ridges, whereas the KN area represents a narrower coastal spread with one or two low elevated, small beach ridges. The inner shelf off the PK area is narrower, whereas the shelf of KN is comparatively wider. Based on the shelf configurations, it is expected that more sediments must have been flushed into the KN coastal area as compared to PK area, where erosion would be greater.

4. Changes in the Landforms

Notable changes occurred along the study area. The entire coastal geomorphology changed and resulted in new landforms which were subjected to dynamic changes during readjustments

with ongoing beach building activities. In many places, it was noted that the steep beaches were converted into gentle ones and vice versa. The behavior of beaches was significantly changed and the response to the post disaster scenario was reversed to that of the earlier time but with quick transformations. Some of the examples are presented below with field illustrations (Figures 2 & 3).



Figure 2 a & b. Pre and Post Tsunami effects at Chandirapadi



Figure 3 a & b. Pre and post tsunami changes at Poompuhar

5. Profiling During Pre- and Post- Tsunami Period

More than 24 beach profiles each for 8 stations along the study area are available for the period during the tsunami. All profiles are mapped. But for the present analysis, pre and post tsunami profiles are discussed here for only three locations viz., Poompuhar (North), Karaikkal (Centre) and Nagoor (South) beaches, where drastic change in profiling are characteristically noticed (Figure 4 a & b).

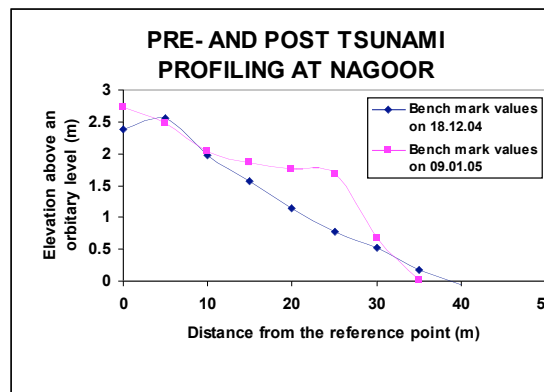
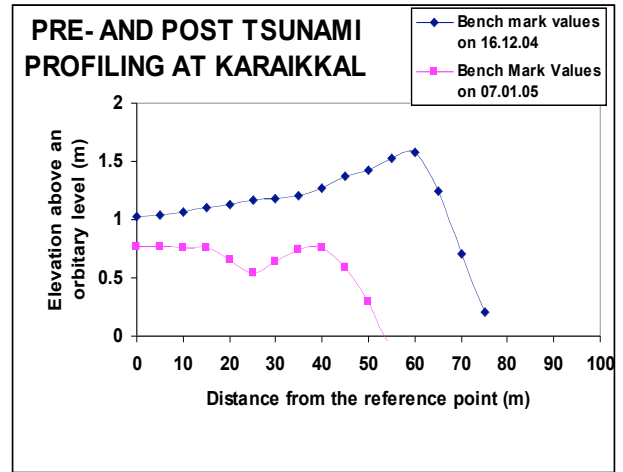
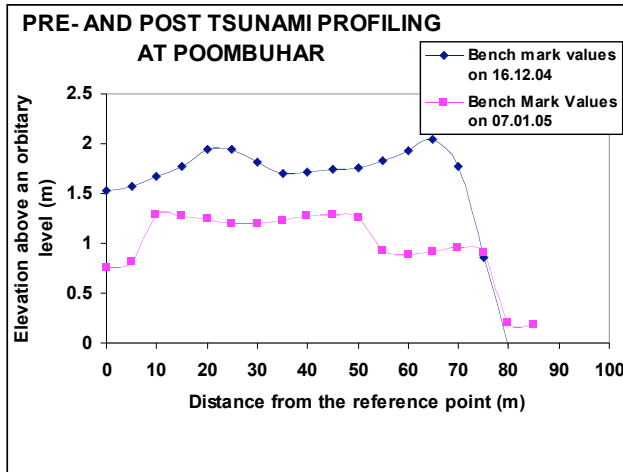
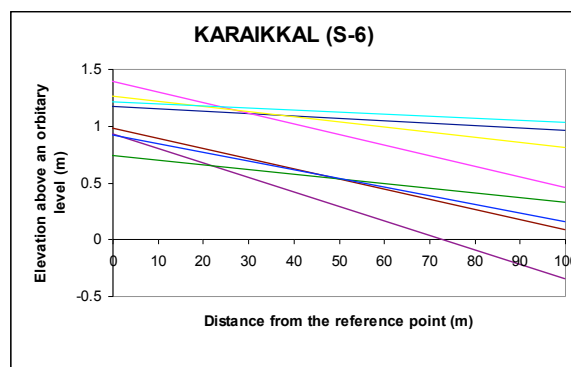
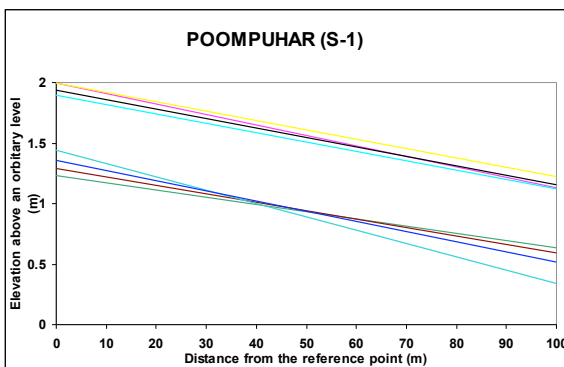


Figure 4 a & b. Pre- and Post-Tsunami Profiling

6. Trend Analysis on Beach Profiling

Beach profiles generated during the pre- and post- tsunami periods were analyzed using linear trend analysis. Pre-tsunami fortnightly profiles (4 Nos.) and Post-tsunami fortnightly profiles (4 Nos.) were studied and details are given in Figure 5a & b. For the purpose of the present discussion, the correlation for Poompuhar, Karaikkal and Nagoor stations are considered.



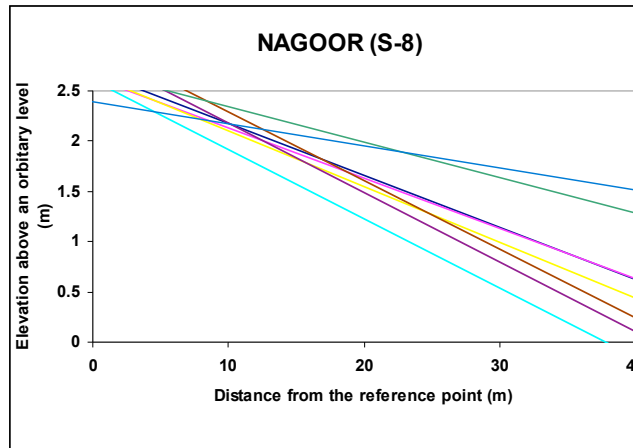


Figure 5 a & b. Trend Analysis

Pre- and post- tsunami trends are smooth at Poompuhar and beach building activity is continuing, whereas sedimentation process at Karaikkal is complex especially after the tsunami. The building capacity is more and severe.

In Nagoor, the trend shows very complex and huge deposition in quick span of time in the post tsunami scenario.

In Nagoor, a meter of deposit occurred in the low tide zone and no erosion in the high tide level. Probably, the drastic change in the deposition at Nagoor may be due to the presence of inlets on either side of the beach. At Karaikkal and Poompuhar strong beach erosion occurred as well as the single inlet and the southern end. Since there was good baseline data for these beaches, the impact of the tsunami was determined accurately. The profile made on the 16th December 2004, as compared to that of 7th January 2005, indicates the value of good baseline data.

The analysis of high tide samples show that the mean values of these sands in the beaches are showing good relation to the strength of erosion. Wherever strong erosion is observed like at the Poompuhar and Karaikkal beaches, a change from fine to medium size sand was observed, whereas at beach like Chinnankudi the sands became finer. The surficial washing must have removed somewhat the coarser sands. The Nagoor beach shows more or less no change in grain size. The high tide region of the beach at Chandirapadi shows a new variety of sand as a result of erosion. Similarly, at Karaikkal beach the complete change in the present surface sands that was observed was caused by the erosion. In all beaches, there was a characteristic shift in the character of the texture of sand between the pre-tsunami and post-tsunami periods (Table 1).

Table 1. Sand textural values of Pre- and Post Tsunami Sediments

Station	Mean	Std.Dev	Skew.	Kurtosis
Poompuhar	2.08(1.64)	0.58(0.44)	0.14(0.10)	1.44(2.85)
Chinnankudi	2.59(3.04)	0.60(0.48)	-0.04(-0.04)	0.94(1.43)
Chandirapadi	2.63(1.99)	0.58(0.65)	-0.02(0.52)	0.95(1.30)
Kottucheri	2.48(2.67)	0.56(0.57)	0.18(-0.10)	1.20(0.91)
Karaikkal	2.59(1.83)	0.58(0.69)	-0.02(0.26)	0.99(1.25)
Nagoor	2.50(2.83)	0.72(0.60)	-0.21(0.06)	0.66(1.01)

Note: Post Tsunami values are given in brackets.

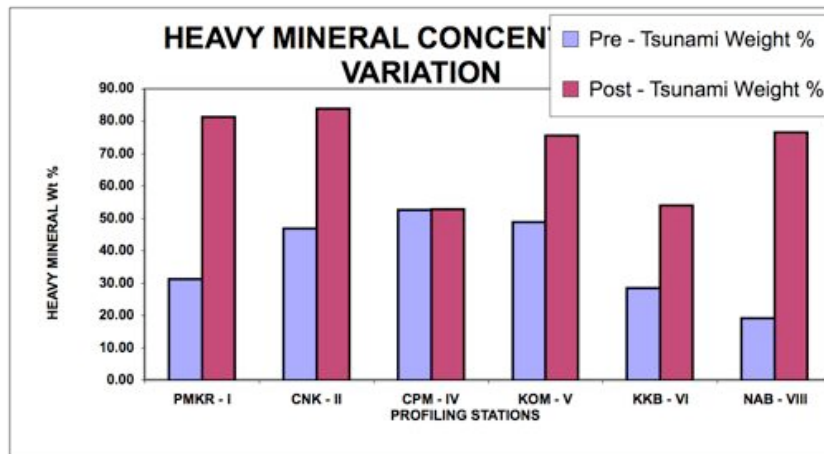


Figure 6. Heavy Mineral deposition scenario

Unlike sediment texture, the heavy mineral analysis showed appreciable changes not only in the concentration but also in the mineral composition. At the Nagoor beach, a dramatic change took place in heavy mineral enrichment. Generally for many years, this beach used to have a 20 % content of heavy minerals. Immediately after the tsunami the heavy mineral compositions was enriched by four times the pre-tsunami level. Moreover, the composition has shown the presence of only garnet, zircon and epidote in the place of fourteen different non-opaque minerals in the assemblage, mainly of flaky constituents (Table 2).

Table 2. Heavy Mineral changes in Weight %

Station Name	Pre – Tsunami Wt %	Post – Tsunami Wt %
Poompuhar	31.10	81.32
Chinnankudi	46.83	83.79
Chandirapadi	52.48	52.79
Kottucherimedu	48.76	75.5.0
Karaikkal	28.25	54.00
Nagoor	19.00	76.45

Whether a beach was erosive or depositive, the heavy mineral concentration has gone to the minimum of twice the strength (Figure 6). The Chandirapadi beach was found to remain an anomaly in maintaining the percentage in tact even after tsunami. However, the composition was found to be without flaky constituents. At Chandirapadi the the impact of the tsunami occurred only at the high tide level segment of the beach.

Detailed studies of the impact of tsunamis on beach sediments may help identify paleo-tsunami material if boreholes are made. In certain places, the concentration of heavier sediments was found to be 2 cm thick. If such thickness with low value of flaky minerals can be found, then such composition may be attributed to deposition by earlier tsunamis.

7. Selective tsunami impacts

Significant Observations

- With all the pre-tsunami beach profiles, it was observed that at least 15 days earlier, there was significant sediment deposition, irrespective of coastline character and behaviour.
- In many locations, the depositional beaches became erosional and vice versa.
- Some of the selected erosional sites became more severely erosional, while at other depositional areas, sediment accretion increased drastically.

The data obtained during pre- and post-tsunami helped assess the selective impacts of the tsunami within a short distance along the shore. Within a coastal distance of 35 km alternate erosion and deposition of sediments were observed. The strong changes in geomorphologic landforms at Poompuhar, associated with the complete removal of the upper sandy layer and its replacement by the lower clay layer suggest the possible influence of inlets in concentrating the tsunami's energy. At the same time, the presence of two inlets on either side neutralizes the tsunami's path and results in the accretion of sediments on the bounded beach. The various changes observed in sediment landforms and mineralogy indicates the possibility of greater impact through the inner-shelf bathymetry. The concentration of heavy minerals indicates that the outer shelf is the source of origin.

Acknowledgements

The authors wish to thank the Honorable Vice-Chancellor of SASTRA University, Thanjavur for encouraging this study. Also, the authors acknowledge with appreciation the Council of Scientific and Industrial Research (CSIR) & the National Resource Data Management System (NRDMS) Division and Earth System Science Division of the Department of Science and Technology (DST) for providing the financial assistance and the necessary equipments to accomplish this study.

REFERENCES

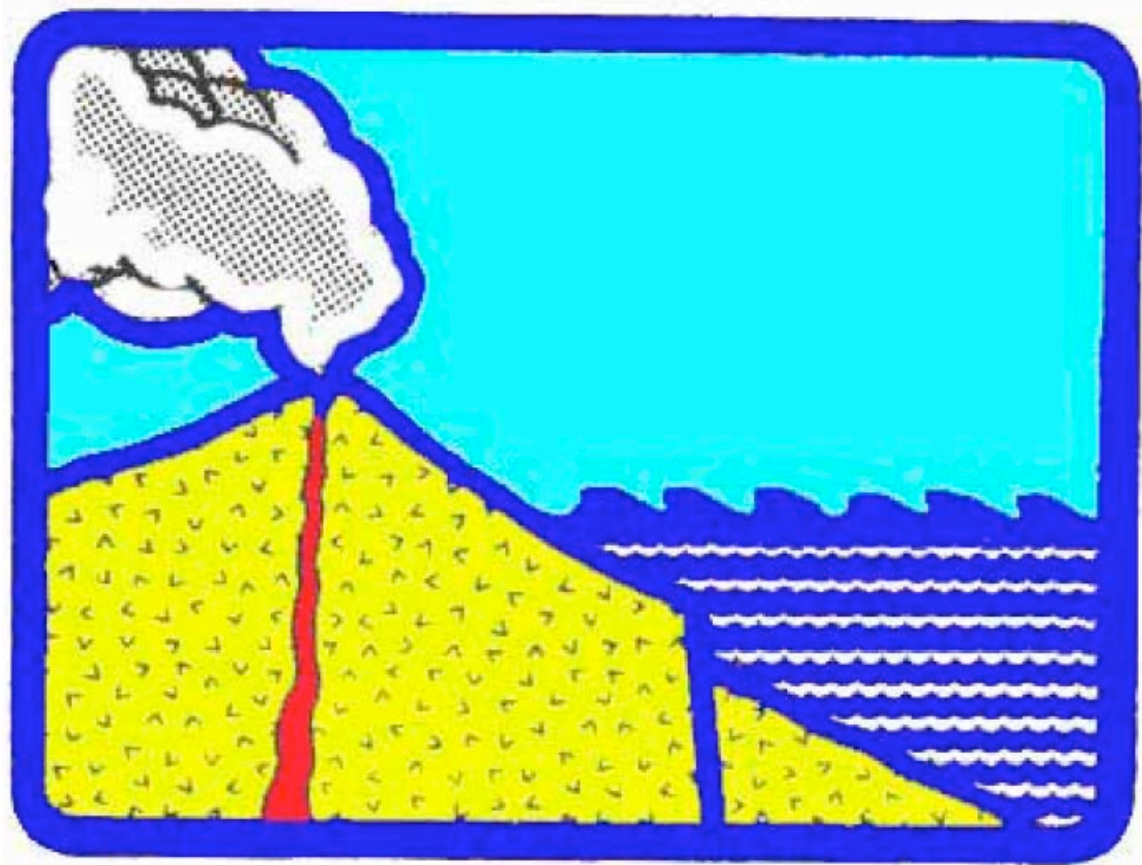
- Clague, J.J, Bobrowsky, P.T., and Hutchinson, I. (2000). A review of geological records of large tsunamis at Vancouver Island, British Columbia, and implications for hazard. *Quaternary Science Reviews*, Vol.19 (9), pp.849-863.
- Dominey-Howes, D, Cundy, A., and Croudace, I. (2000). High energy marine flood deposits on Astypalaea Island, Greece: possible evidence for the AD 1956 southern Aegean tsunami. *Marine Geology*, Vol.163 (1-4), pp.303-315.
- Heck, 1947. List of seismic sea waves. *Bulletin of the Seismological Society of America*, 37(4):269-286.
- Iida, Kumizi, Doak C. Cox, and George Pararas-Carayannis, 1967. Preliminary Catalog of Tsunamis Occurring in the Pacific Ocean, HIG-67-10, Hawaii Institute of Geophysics, University of Hawaii, Honolulu, Hawaii, 275 p. Bibliography to the Preliminary Catalog of Tsunamis Occurring in the Pacific Ocean, December 1967, 27 p.
- Lander, J.F. and Whiteside, L.S., 1997. Caribbean tsunamis: an initial history, http://rmoclis.upr.clu.edu/tsunamis/Lander/J_Lander.html.
- Maramai, A., Graziani, L., and Tinti, S. (2005). Tsunamis in the Aeolian Islands (southern Italy): a review. *Marine Geology*, Vol.215 (1-2), pp. 11-21.
- McMurtry, G.M., Watts, P., Fryer, G.J., Smith, R. and Imamura, F. (2004). Giant landslides, mega-tsunamis, and paleo-sea level in the Hawaiian Islands. *Marine Geology*, Vol. 203 (3-4), pp.219-233.
- Monge, J. and Mendoza, J., (1993). Study of the effects of tsunami on the coastal cities of the region of Tarapacá, north Chile. *Tectonophysics*, Vol. 218 (1-3), pp.237-246.
- Mörner, N. A., (1999). Paleo-tsunamis in Sweden. *Physics and Chemistry of the Earth, Part B: Hydrology, Oceans and Atmosphere*, Vol. 24 (5), pp. 443-448.
- Nakata, I., Kawana, A., Nakatsuji, N., 1993. Perpendicular contact guidance of CNS neuroblasts on artificial microstructures. *Development* **117**: 401OE408
- Nanayama.F, Shigeno.K, Satake.K, Shimokawa.K, Koitabashi.S, Miyasaka.S and Ishii.M (2000) Sedimentary differences between the 1993 Hokkaido-nansei-oki tsunami and the 1959 Miyakojima typhoon at Taisei, southwestern Hokkaido, northern Japan. *Sedimentary Geology*, Vol.135 (1-4) pp. 255-264.
- NGDC, 2001. Tsunami Database at National Geophysical Data Center, URL: <http://www.ngdc.noaa.gov/seg/hazard/tsu.shtml>.

Papadopoulos, G. A., and B. J. Chalkis. B. J., (1984). Tsunamis observed in Greece and the surrounding area from antiquity up to the present times. *Marine Geology*, Vol.56 (1-4), pp.309-317.

Scheffers, A. and Kelletat, D., (2003). Sedimentologic and geomorphologic tsunami imprints worldwide—a review. *Earth-Science Reviews*, Vol. 63 (1-2), pp. 83-92.

Shi, S., Dawson, A.G. and Smith, D.E., 1995. Coastal Sedimentation Associated with the December 12th, 1992 Tsunami in Flores, Indonesia, *Pure and Applied Geophysics*, Vol. 144, No. 3-4, pp. 525-536.

Tappin, D. R., Watts, P., McMurtry, G. M, Lafoy, Y. and Matsumoto, T. (2001). The Sissano, Papua New Guinea tsunami of July 1998 - offshore evidence on the source mechanism. *Marine Geology*, Vol.175 (1-4), pp.1-23.



Copyright © 2008

**The Tsunami Society
P. O. Box 2117
Ewa Beach, HI 96706-0117, USA**

WWW.TSUNAMISOCIETY.ORG